AMERICAN SOCIETY FOR MICROBIOLOGY | mSystems®

RESEARCH ARTICLE

Global Chromosome Topology and the Two-Component Systems in Concerted Manner Regulate Transcription in *Streptomyces*

Martyna Gongerowska-Jac,[a] Marcin J. Szafran,[a] Jakub Mikołajczyk,[a] Justyna Szymczak,[a] Magdalena Bartyńska,[a] Anna Gierlikowska,[a] Sylwia Biały,[a] Marie A. Elliot,[b] Dagmara Jakimowicz[a]

[a]Faculty of Biotechnology, University of Wrocław, Wrocław, Poland
[b]Department of Biology, McMaster University, Hamilton, Ontario, Canada

ABSTRACT Bacterial gene expression is controlled at multiple levels, with chromosome supercoiling being one of the most global regulators. Global DNA supercoiling is maintained by the orchestrated action of topoisomerases. In *Streptomyces*, mycelial soil bacteria with a complex life cycle, topoisomerase I depletion led to elevated chromosome supercoiling, changed expression of a significant fraction of genes, delayed growth, and blocked sporulation. To identify supercoiling-induced sporulation regulators, we searched for *Streptomyces coelicolor* transposon mutants that were able to restore sporulation despite high chromosome supercoiling. We established that transposon insertion in genes encoding a novel two-component system named SatKR reversed the sporulation blockage resulting from topoisomerase I depletion. Transposition in *satKR* abolished the transcriptional induction of the genes within the so-called supercoiling-hypersensitive cluster (SHC). Moreover, we found that activated SatR also induced the same set of SHC genes under normal supercoiling conditions. We determined that the expression of genes in this region impacted *S. coelicolor* growth and sporulation. Interestingly, among the associated products is another two-component system (SitKR), indicating the potential for cascading regulatory effects driven by the SatKR and SitKR two-component systems. Thus, we demonstrated the concerted activity of chromosome supercoiling and a hierarchical two-component signaling system that impacts gene activity governing *Streptomyces* growth and sporulation.

IMPORTANCE *Streptomyces* microbes, soil bacteria with complex life cycle, are the producers of a broad range of biologically active compounds (e.g., antibiotics). *Streptomyces* bacteria respond to various environmental signals using a complex transcriptional regulation mechanism. Understanding regulation of their gene expression is crucial for *Streptomyces* application as industrial organisms. Here, on the basis of the results of extensive transcriptomics analyses, we describe the concerted gene regulation by global DNA supercoiling and novel two-component system. Our data indicate that regulated genes encode growth and sporulation regulators. Thus, we demonstrate that *Streptomyces* bacteria link the global regulatory strategies to adjust life cycle to unfavorable conditions.

KEYWORDS DNA supercoiling, *Streptomyces*, sporulation, topoisomerases, transcription factors, transcriptional regulation, two-component system

In all organisms, gene expression is precisely controlled, primarily at the level of transcription initiation. The main transcriptional regulatory factors include promoter DNA sequences and *trans*-acting transcriptional regulators. Bacterial genomes encode numerous transcriptional regulators, among which the key players are DNA-binding

Editor Gilles P. van Wezel, Leiden University

Address correspondence to Martyna Gongerowska-Jac, martyna.gongerowska-jac@uwr.edu.pl, or Dagmara Jakimowicz, dagmara.jakimowicz@uwr.edu.pl.

Received 15 September 2021
Accepted 31 October 2021
Published 16 November 2021

proteins like sigma factors, which recruit RNA polymerase (RNAP) to promoters, and transcription factors (TFs), which may act as repressors or activators by affecting RNAP binding (1, 2). Notably, the binding of regulatory proteins in bacteria is in turn controlled by systems that adjust transcription in response to external and internal cell conditions. Examples include changes in chromosome topology to modify promoter accessibility to regulatory factors, as well as the modification of regulatory protein activity itself (3).

The activity of specific sigma factors or regulatory proteins can be modulated through partner protein or ligand binding, as well as through proteolysis or covalent modifications like phosphorylation. The importance of phosphorylation has been well established for regulators that are a part of two-component systems (TCSs). Canonical TCSs consist of a transmembrane sensor histidine kinase (HK) and cytoplasmic response regulator (RR), which detects environmental signals and triggers intracellular responses, respectively (4). Upon signal sensing, the kinase in classical TCSs undergoes autophosphorylation and subsequently transfers the phosphate moiety to its cognate response regulator, which promotes DNA binding and transcriptional control of its target genes. While the regulatory targets and biological functions of many regulatory proteins have been well described (5), a plethora of them remain unexplored.

One of the crucial factors influencing regulatory protein binding to DNA is chromosome topology, determined by chromosome supercoiling and nucleoid-associated proteins (NAPs). The global chromosome topology of bacteria depends on growth phase and environmental conditions and adjusts transcription in response to both extra- and intracellular conditions. Overall, bacterial chromosome supercoiling is controlled by enzymes called topoisomerases, mainly the TopA type I topoisomerase, which relaxes DNA (removes negative supercoils), and gyrase, which in contrast introduces negative supercoils (6). Inhibiting topoisomerase activity or altering topoisomerase levels leads to changes in chromosome topology and affects DNA transactions, including replication and transcription. To date, studies on various bacterial species (*Streptococcus pneumoniae*, *Haemophilus influenzae*, *Escherichia coli*, *Salmonella enterica*, and *Streptomyces coelicolor*) have shown that disturbances in the topological balance affect the transcription of a significant fraction of so-called supercoiling-sensitive genes (7–13).

The binding of NAPs also depends on chromosome topology, with NAPs in turn affecting the binding of other transcription factors (3, 14–18). However, little is known about the cross talk between chromosome supercoiling and other regulatory systems controlling gene transcription, particularly in response to changes in environmental conditions.

Soil-dwelling bacteria such as *Streptomyces* frequently encounter environmental stress. *Streptomyces* adaptations to the soil environment include their mycelial growth and complex developmental life cycle, which encompasses both spore formation and exploratory growth (19, 20). Vegetatively growing *Streptomyces* cells elongate and branch to generate a network of multicellular hyphae. In response to environmental stimuli, particularly nutrient depletion, sporulation is triggered. Sporulation starts with raising aerial hyphae, within which spore chains subsequently develop. The conversion of multigenomic hyphal cells to chains of unigenomic spores requires chromosome condensation and segregation, accompanied by synchronous septation (19, 21). The progression of the *Streptomyces* life cycle is governed by a set of well-described regulatory proteins (such as those encoded by the *whi* or *bld* genes) (22, 23); however, numerous reports indicate an abundance of less-studied regulators and other proteins that also contribute to sporulation regulation (24–29).

Streptomyces bacteria use a repertoire of biologically active secondary metabolites to thrive in their environmental niche, including numerous antibiotics (approximately 60% of natural antibiotics are produced by *Streptomyces*), immunosuppressants, and cytostatics (30). The production of secondary metabolites remains under the control of complex regulatory networks and is coordinated with developmental programs (31–34). As a free-living organism, *Streptomyces* responds to highly variable conditions using a large number of transcriptional regulators, many of which remain

uncharacterized (31). The number of transcription factors encoded by streptomycete genomes ranges from 471 to 1,101, and among these, depending on the species, there are 315 to 691 transcriptional regulators and 31 to 76 sigma factors (26). Compared to other bacterial genera, *Streptomyces* genomes also encode numerous TCSs, the number of which varies depending on the species, ranging from 59 and 117, alongside 13 to 21 orphan response regulators and 17 to 39 unpaired/uncharacterized sensor kinases (35–37).

As in other bacteria, chromosome topology plays a critical role in the regulation of gene expression in *Streptomyces*. In contrast to many bacteria, the model *Streptomyces* species *S. coelicolor* possesses only one type I topoisomerase, TopA, which is essential for viability (38). TopA depletion in *Streptomyces* results in increased DNA supercoiling and altered gene expression, leading to severe growth retardation and sporulation blockage (38, 39). Moreover, disturbances in global DNA supercoiling affect the transcription of up to 7% of *Streptomyces* genes (12). Numerous supercoiling-sensitive genes are grouped into discrete clusters, with one cluster in particular, named SHC (supercoiling-hypersensitive cluster), exhibiting extreme DNA supercoiling sensitivity. This region encodes many proteins of unassigned function but also appears to include a two-component system, anti-sigma factors and probable transcriptional regulators. Interestingly, most of the SHC genes are poorly transcribed under standard conditions but are upregulated in response to increased DNA supercoiling (12). Having established that altered DNA supercoiling significantly impacts transcription in *S. coelicolor*, we predicted that altered gene expression may contribute to the sporulation inhibition observed for the TopA-depleted strain.

To identify the genes responsible for sporulation and growth inhibition under high supercoiling conditions, we performed random transposon mutagenesis of the TopA-depleted *S. coelicolor* strain and screened for strains with mutations that suppressed the sporulation blockage associated with high DNA supercoiling. We found that mutations in genes encoding a two-component system named SatKR (SCO3390-89) led to altered transcription of the SHC cluster. We established that the activated response regulator SatR (SCO3389) inhibited growth and sporulation by inducing transcription of SHC genes independently of high DNA supercoiling. Moreover, we confirmed that mutations within SHC prevented the activation of genes within this region and restored growth and sporulation to the TopA-depleted strain. Thus, our results reveal a unique interplay between the two-component system SatKR and chromosome supercoiling in regulating SHC gene expression, with the SHC products subsequently impacting *S. coelicolor* growth and sporulation.

RESULTS

Screening for suppressors of supercoiling-induced sporulation blockage. TopA is the only type I *S. coelicolor* topoisomerase and consequently is essential for viability. Its depletion in the TopA-controlled strain (PS04, in which the *topA* gene expression is under the control of the thiostrepton-inducible promoter *tipA*, allowing for an up to 20-fold depletion of TopA levels) leads to increased negative DNA supercoiling (38). Elevated negative DNA supercoiling in turn results in changes in global gene expression and affects the growth rate, sporulation, and secondary metabolism of *S. coelicolor* (12, 38). During differentiation of wild-type *S. coelicolor*, white sporogenic (aerial) hyphae mature into chains of gray spores; in contrast, the development of a TopA-depleted strain is inhibited at the aerial hyphal stage, resulting in a "white colony phenotype." We speculated that inhibition of aerial hypha maturation may result from changes in the expression of supercoiling-sensitive genes encoding sporulation regulators (12). To identify any such sporulation regulators, we searched for transposon mutations that were able to suppress the TopA depletion phenotype and restore sporulation (gray colonies). To ensure that the transposon insertion frequency was sufficient to cover all 7,825 predicted *S. coelicolor* genes (40), we aimed to obtain a mutant library containing approximately 16,000 clones. Having obtained the representative

transposon library (PS04-Tnlib), we searched for mutants that formed gray colonies under TopA-depleted conditions. We identified seven transposants exhibiting this phenotype, and among them, one transposant, termed MGHM5, additionally exhibited a partially restored growth rate upon TopA depletion (with effective depletion being confirmed by Western blotting and reverse transcription-quantitative PCR [RT-qPCR]; see Fig. S1 in the supplemental material), both on solid medium and in liquid medium, compared with its TopA-depleted parental strain (Fig. 1A and B). Unlike the TopA-depleted parental strain, which overproduced blue actinorhodin, the TopA-depleted transposon strain did not produce either of the pigmented antibiotics made by *S. coelicolor* (blue actinorhodin or red undecylprodigiosin) (Fig. 1A). Microscopic analysis of spores produced by the TopA-depleted transposon strain confirmed the presence of spore chains, although these were detectable only after prolonged incubation (approximately 53 h compared to the 48 h needed to sporulate in the wild-type strain, Fig. 1C); spore chains could not be detected in the TopA-depleted parental strain (Fig. S2). Interestingly, the spores produced by the TopA-depleted transposon strain were of various sizes compared with the wild-type strain and the parental strain in which the TopA level was restored to that of the wild-type strain (PS04, 1 μg/ml thiostrepton). Moreover, spores produced by the TopA-depleted transposon strain were highly sensitive to 5% sodium dodecyl sulfate (SDS): only 2.5% survived 1 h of SDS exposure compared with the 76% spore survival of the same strain with restored TopA levels (Fig. 1D).

Next, we tested whether the increased growth rate and sporulation of the TopA-depleted transposon strain resulted from a restoration of wild-type levels of chromosome supercoiling. To achieve this goal, we isolated a supercoiling reporter plasmid (pWHM3Hyg) from a derivative of the TopA-depleted transposon strain (MGHM5_RP) and established that its negative supercoiling level was similar to that of plasmid isolated from the parental TopA-depleted strain derivative, indicating similar chromosome supercoiling (Fig. 1E).

Thus, we successfully identified a transposon mutant in which sporulation and growth rate defects of the parental TopA-depleted strain were restored to wild-type levels, and the observed phenotypic effect did not result from restored negative supercoiling.

Transposon insertion in two-component system-encoding genes influences the expression of a supercoiling-sensitive cluster. We mapped the transposon insertion loci in the MGHM5 strain (by sequencing rescue plasmids and genome sequencing), identifying two transposons: one in *sco3390* and one in *sco2474*. In both cases, the orientation of the *aadA(1)* gene within the transposon cassette was the same as that of the disrupted gene. In the first locus (*sco3390*), the transposon cassette was inserted 292 nucleotides downstream of the start codon (Fig. 2). The *sco3390* gene (1,206-bp length) was annotated as encoding a putative two-component system kinase, while the genes downstream of this, in a presumable operon, were annotated as encoding a probable cognate response regulator (*sco3389*) and TrmB-like protein (*sco3388*) (41, 42). The second transposition site was located 1,020 nucleotides downstream of the start codon of the *sco2474* gene (1,644 bp in length), which encodes a putative secreted metalloproteinase (Fig. S3A). Importantly, previously performed transcriptome sequencing (RNA-seq) analysis (12) showed that while the *sco3388-3390* genes were transcribed during *S. coelicolor* vegetative growth in a supercoiling-insensitive manner (Fig. 3A, left panel), the *sco2474* gene was not expressed during vegetative growth, either in normal or in high DNA supercoiling conditions (i.e., in the TopA-depleted PS04 strain) (Fig. S3B). Moreover, *sco2475*, located downstream of the disrupted gene, was transcribed in the transposon strain, and its expression was not changed due to transposition, suggesting a lack of polar effects associated with this transposon insertion (Fig. S3B). Since *sco2474* was not expressed under any tested conditions, and we knew that transposition in MGHM5 affected not only sporulation but also the vegetative growth rate, we excluded the disruption of *sco2474* as a reason for the restored growth of the TopA-depleted transposon strain and focused our attention on the *sco3390* gene/operon.

Transposon insertion in the kinase-encoding *sco3390* gene was expected to affect the level of expression of the downstream response regulator-encoding *sco3389* gene.

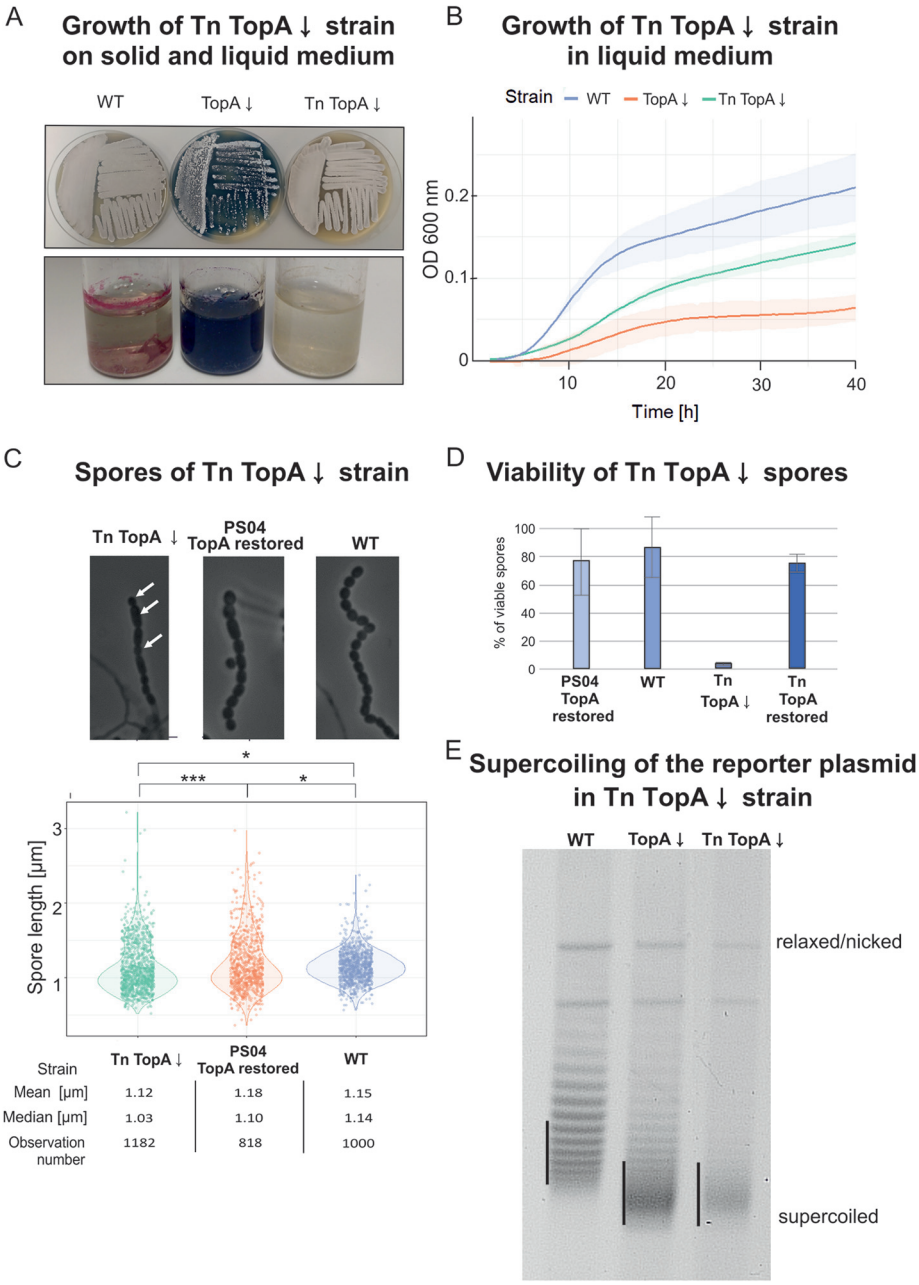

FIG 1 Phenotype of the TopA-depleted transposon strain MGHM5 (Tn TopA↓). (A) Growth of the TopA-depleted transposon strain (Tn TopA↓) on solid MS agar (top panel) and antibiotic production in R2 liquid medium (bottom panel) compared with wild-type (WT) and TopA-depleted PS04 (TopA↓) strains. The cultures were grown for 72 h. (B) Growth curves of the TopA-depleted transposon strain (Tn TopA↓) in liquid 79 medium compared with WT and TopA-depleted PS04 (TopA↓) strain growth. The growth rate was measured in triplicate using a Bioscreen C instrument for 48 h. (C) Spores produced by the TopA-depleted transposon strain (Tn TopA↓). (Top) Phase-contrast microscopy images demonstrating representative spore chains of the TopA-depleted transposon strain (Tn TopA↓) and its parental strain PS04 with restored TopA levels (induced with 1 μg/ml thiostrepton) and the wild-type strain after 53 h of growth in MM minimal medium (with 1% mannitol). (Bottom) Spore size distribution. Asterisks indicate the significance of the *P* value (*, $P \leq 0.05$; ***, $P \leq 0.001$) when comparing mean spore sizes. (D) Viability of spores of the TopA-depleted transposon strain (Tn TopA↓) after SDS treatment compared with the wild-type strain, PS04 with restored TopA levels, and transposon strain (Tn) with TopA level restored. Spores were collected and incubated for 1 h in 5% SDS at room temperature. The viability percentage was calculated as a ratio of the colony number grown from spores treated and untreated with disrupting agent. (E) DNA supercoiling of the reporter plasmid pWHM3Hyg or pWHM3Spec isolated from the wild-type strain derivative MS10 (WT), TopA-depleted strain derivative MS11 (TopA↓) and TopA-depleted transposon strain derivative (MGHM5_RP, Tn TopA↓) cultured for 24 h in liquid 79 medium. The distribution of the reporter plasmid topoisomers was analyzed by agarose gel electrophoresis. Black vertical lines indicate the most abundant topoisomers.

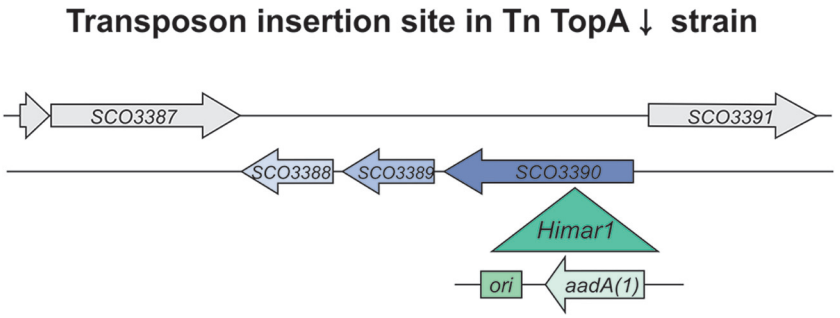

FIG 2 Position of the *Himar1* transposon insertion site in the MGHM5 strain. The green triangle shows the insertion site within the *sco3390* gene with the orientation of the inserted *aadA(1)* gene. *ori*, origin of replication.

Moreover, since the transposon insertion was expected to inactivate the kinase-encoding gene, we further predicted that this mutation would modify the phosphorylation state and activity of its cognate regulator. Transcriptional analysis (RNA-seq, confirmed by RT-qPCR analysis) performed on RNA isolated from liquid cultures of the TopA-depleted MGHM5 transposon strain showed significant *sco3389* downregulation compared with the parental TopA-depleted strain (Fig. 3A and Fig. S4). Additionally, we established that the expression of 100 genes changed significantly in the TopA-depleted MGHM5 transposon strain compared to its parental TopA-depleted strain. The majority of differentially expressed genes (72 genes) were downregulated in the transposon mutant, with only 28 genes being upregulated compared to the parental TopA-depleted strain (Data Set S1, Tab 1; Fig. 3B, left panel). Surprisingly, 30 of 72 downregulated genes were concentrated in one region of the chromosome: the supercoiling-hypersensitive cluster (SHC) encompassing 34 genes (*sco4667-sco4700*). The majority of the SHC genes (26 of 34 genes) have been previously shown to not be transcribed or transcribed at very low levels under optimal growth conditions but highly induced upon TopA depletion (12) (Fig. 3B, right panel, and Fig. 3C). We confirmed the decreased transcription of SHC genes in the TopA-depleted transposon strain compared with the TopA-depleted parental strain using RT-PCR with primers specific for the first (*sco4667*) and penultimate gene (*sco4699*) of the SHC cluster (Fig. 3D). According to the RT-qPCR results, SHC gene expression was reduced despite TopA depletion, although not to the extent observed in the RNA-seq analysis, which might be due to the different approaches to measure the transcript levels (over the whole gene length versus in a certain position).

In summary, we determined that our TopA-depleted strain carrying a transposon integrated into *sco3390* exhibited an altered transcriptional landscape compared with its parent TopA-depleted strain, with reverted induction of the supercoiling-sensitive SHC genes. This implicated the *sco3389-sco3390*-encoding two-component system in controlling the transcription of the supercoiling-sensitive cluster and led us to term these gene products SatKR (for SHC activity controlling two-component system kinase/regulator).

Changes in SatKR levels affect *Streptomyces* growth and sporulation. To confirm that the SatKR two-component system regulated growth and sporulation in *S. coelicolor* in coordination with chromosome supercoiling, we analyzed the phenotypic effects of *satKR* gene deletion and *satR* overexpression in different genetic backgrounds.

Unexpectedly, deleting *satKR* did not affect vegetative growth in liquid medium or differentiation on solid medium in either the wild-type or TopA-depleted backgrounds (MGM12 and MGP12 strains, respectively) compared to parental strains (Fig. 4A). Sporulation of the Δ*satKR* mutant was also unaffected in the wild-type background, while in the TopA-depleted background, sporulation was not restored, based on plate analyses, and was confirmed microscopically (Fig. S5). Thus, eliminating both

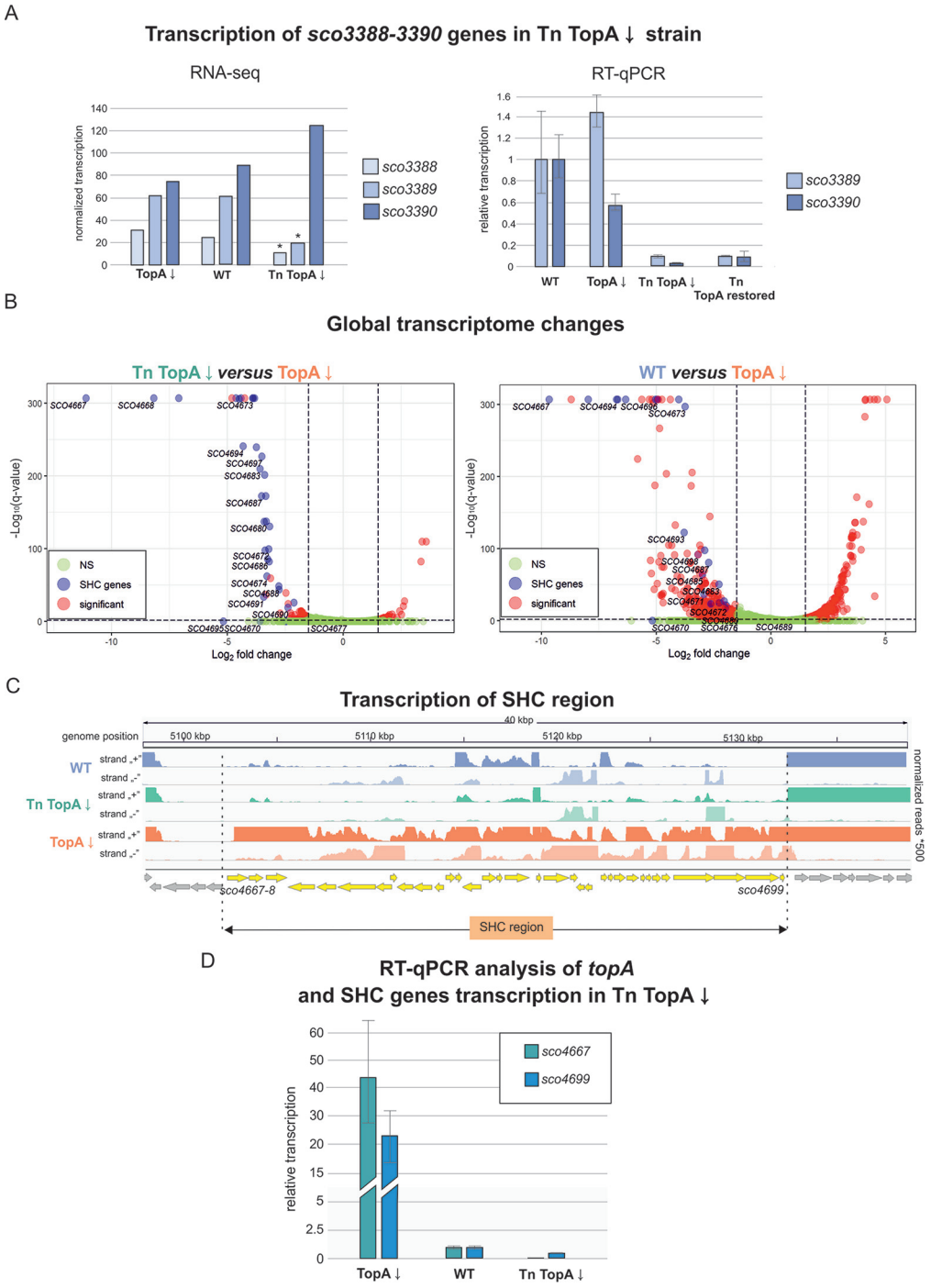

FIG 3 Transcriptional changes in the TopA-depleted transposon mutant MGHM5 (Tn TopA↓) compared with its TopA-depleted parental strain (PS04) and wild-type strain. (A) Normalized transcription level of *sco3390-sco3388* genes in the TopA-depleted transposon strain (Tn TopA↓), transposon strain with TopA level restored (Tn TopA restored), its parental TopA-depleted PS04 strain (TopA↓), and the wild type (WT), based on RNA-seq (left) and the relative transcription level analyzed by RT-qPCR (right). Asterisks in the RNA-seq analysis indicate statistical significance of the q value and $\log_2$ fold ($q \leq 0.01$ and $1.5 < \log_2$ fold < -1.5). (B) Volcano plots based on the RNA-seq experiments showing changes in global gene expression in the TopA-depleted transposon strain (Tn TopA↓ strain) compared with its parental TopA-depleted PS04 strain (TopA↓) (left), as well as genes affected by supercoiling (changes between the wild-type strain and TopA-depleted PS04 strain [TopA↓]) (right panel, data obtained earlier [12]). Significantly altered transcripts ($q \leq 0.01$ and $1.5 < \log_2$ fold < -1.5) are depicted in red, SHC genes are shown in blue, and genes with unchanged transcription are marked in green. NS, not significant. (C) Transcriptional profile of the SHC region in the wild-type strain (blue), TopA-depleted transposon mutant (Tn TopA↓; green) and TopA-depleted parental PS04 strain (TopA↓; orange). SHC genes are depicted in yellow. (D) Silencing of SHC gene transcription in the TopA-depleted transposon strain (Tn TopA↓) compared with its parental TopA-depleted PS04 strain (TopA↓) and wild-type strain analyzed by RT-qPCR. Primers for amplification of the two genes, the first and last genes of the SHC cluster (*sco4667* and *sco4699*), were used.

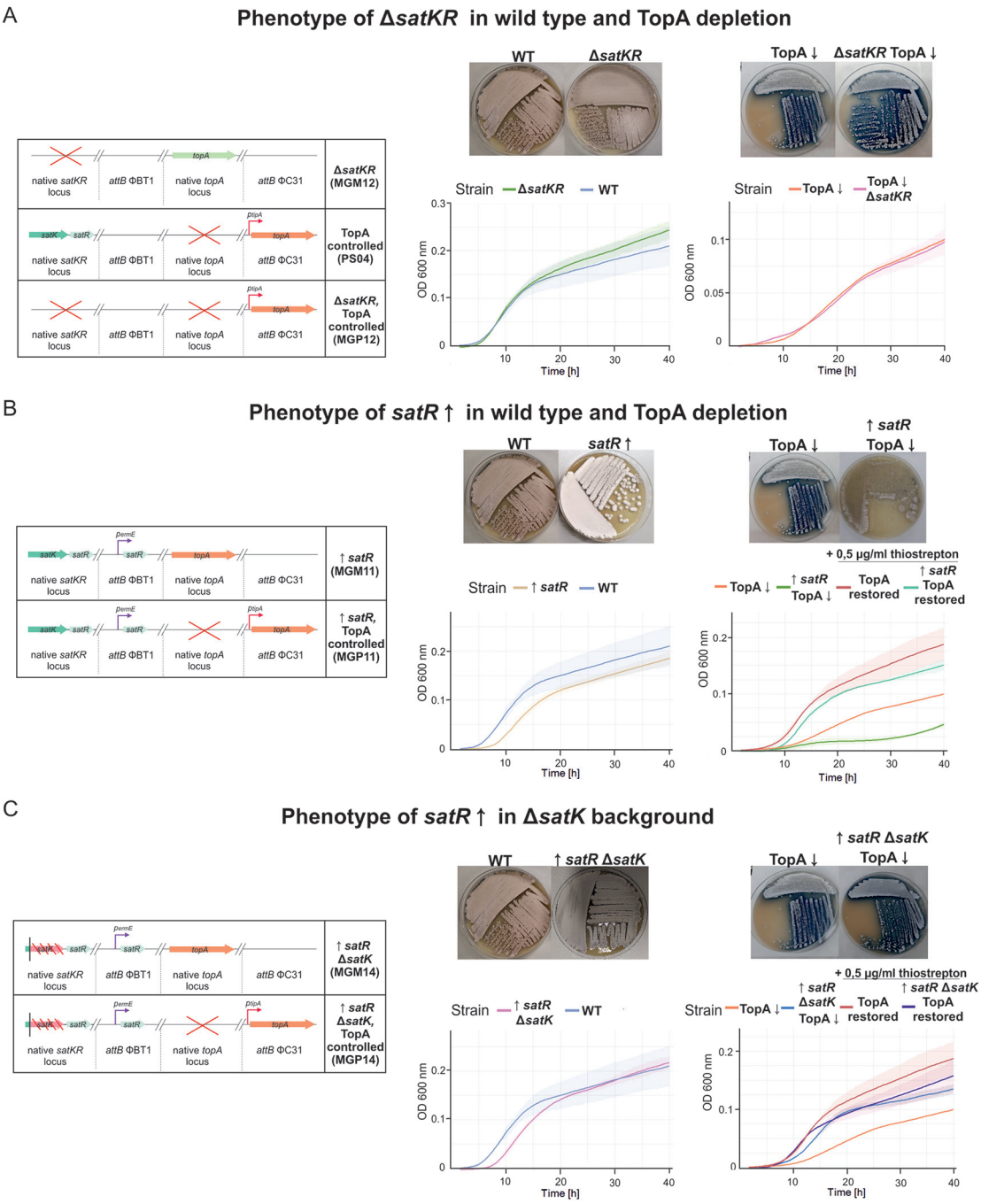

FIG 4 Phenotypes of *satKR* mutant strains. (A) The phenotype of the MGM12 strain with *satKR* deletion in the wild-type background (Δ*satKR*) and the MGP12 strain carrying the *satKR* deletion in the TopA-controlled background (TopA-depleted Δ*satKR* TopA↓ and TopA restored with the addition of 0.5 μg/ml thiostrepton inducer [Δ*satKR* TopA restored]). (Left) Scheme of the mutant strain genotypes. (Right, top) Growth and differentiation of strains carrying the Δ*satKR* deletion in the wild-type and TopA-depleted background on MS agar after 48 and 72 h of growth, respectively. (Bottom) Growth curves in liquid 79 broth obtained using a Bioscreen C instrument. Measurements were performed in triplicate every 20 min for 42 h. (B) The phenotype of strain MGM11 overexpressing *satR* in the wild-type background (*satR*↑) and strain MGP11 overexpressing *satR* in the TopA-controlled background (TopA-depleted: *satR*↑TopA↓ and TopA restored with the addition of 0.5 μg/ml thiostrepton inducer: *satR*↑ TopA restored). (Left) Scheme of the mutant strain genotypes. (Right, top) Growth and differentiation of the analyzed strains on MS agar after 48 or 72 h of growth, respectively. (Bottom) Growth curves of the analyzed strain in liquid 79 broth obtained using a Bioscreen C instrument. Measurements were performed in triplicate every 20 min for 42 h. (C) The phenotype of the MGM14 strain overexpressing *satR* in the *satK* deletion background (*satR*↑Δ*satK*) and the MGP14 strain overexpressing *satR* in the TopA-controlled *satK* deletion background (TopA depleted: *satR*↑Δ*satK* TopA↓ or TopA restored with the addition of 0.5 μg/ml thiostrepton inducer: *satR*↑Δ*satK* TopA restored). (Left) Scheme of the mutant strain genotypes. (Right, top) Growth of analyzed strains on MS agar for 48 or 72 h. (Bottom) Growth curves of the analyzed strain in liquid 79 broth obtained using a Bioscreen C instrument. Measurements were performed in triplicate every 20 min for 42 h.

components of the SatKR system had different phenotypic effects than the inactivation of the SatK kinase and lowering of the *SatR* transcript levels in transposon strains.

To further explore the role of SatR, we overexpressed *satR* in the presence of its cognate kinase (using an additional copy of the *satR* gene under the control of a strong constitutive p_{ermE} promoter, with overexpression being confirmed using RNA-seq and RT-qPCR analysis [Fig. S6]) in both the wild-type strain and the TopA-controlled strain (MGM11 and MGP11 strains, respectively; Fig. 4B). Elevated *satR* transcription slightly retarded vegetative growth in liquid cultures and delayed differentiation on solid medium in both the wild-type and TopA-depleted backgrounds compared to the parental strains (Fig. 4B and Fig. S5). Moreover, the *satR*-overexpressing strain with restored TopA levels exhibited somewhat inhibited growth compared with the TopA-restored parental strain (Fig. 4B). These observations suggested that overexpression of *satR* in the presence of the cognate kinase SatK impaired cell growth.

To assess the importance of its cognate kinase on SatR activity, we inactivated *satK* by frameshift mutation in the wild-type and TopA-controlled backgrounds and overexpressed *satR* in the obtained strains (MGM14 and MGP14 strains, respectively). In contrast to *satR* overexpression in the presence of kinase, elevated *satR* transcript levels in the absence of cognate kinase did not affect the growth rate and development either in liquid medium or on solid medium (Fig. 4C) compared with the parental strains. These observations suggested that SatK was crucial for SatR activity and its influence on growth and sporulation.

In summary, overexpression of *satR* in the presence of its intact cognate kinase gene (*satK*) led to growth inhibition and delayed sporulation; these effects were lost when *satK* was inactivated.

The SatKR regulon includes SHC genes. To better understand the biological function of SatKR, we investigated how modulating *satKR* gene expression in different genetic backgrounds affected global gene transcription.

Transcriptional analysis showed that deletion of *satKR* in the wild-type background (MGM12) altered the expression of 126 genes (1.5% of all *S. coelicolor* genes) (see Data Set S1, Tab 2, in the supplemental material). Within these genes, there were nine SHC genes (seven of which were supercoiling sensitive), which we observed to be further downregulated in the *satKR* mutant (despite their very low expression in the wild type), indicating that the SatKR system also influenced the expression of the SHC genes under normal supercoiling conditions. Changes in gene expression were also observed when *satKR* was deleted in the TopA-depleted background (strain MGP12), where 67 genes, or 0.76% of all *S. coelicolor* genes, had significantly altered expression (Data Set S1, Tab 3 and Tab 4). However, the expression of SHC genes activated by high DNA supercoiling in this mutant was unaffected, indicating that the presence of SatR and absence of SatK (as in the transposon mutant) are required for this inhibition.

Next, we established the impact of *satR* overexpression on transcription in the wild-type and TopA-depleted backgrounds (MGM11 and MGP11 strains, respectively). We determined that a high level of SatR in the presence of SatK under normal supercoiling conditions significantly affected the expression of 452 genes (approximately 5% of all genes) (Data Set S1, Tab 5). Among these genes, 351 (nearly 78%) were activated due to *satR* upregulation, while the expression of 101 genes was reduced (Fig. 5A). A similar effect was noted in the TopA depletion background (Data Set S1, Tab 6, 409 genes with altered transcription); however, only 55 genes were equally changed in both wild-type and TopA-depleted conditions. *satR* overexpression in the presence of SatK and normal DNA supercoiling (MGM11) was also found to activate the transcription of 16 genes from the SHC region (Fig. 5B). We confirmed the activation of *sco4667* (first SHC gene) and *sco4699* (penultimate SHC gene) using RT-qPCR (Fig. 5C). In the TopA-depleted background (MGP11 strain), *satR* overexpression did not significantly affect SHC transcription (with one exception being *sco4677*), as under high DNA supercoiling conditions, the transcription of these genes was already highly induced.

While overexpression of SatR in the presence of the SatK kinase activated numerous

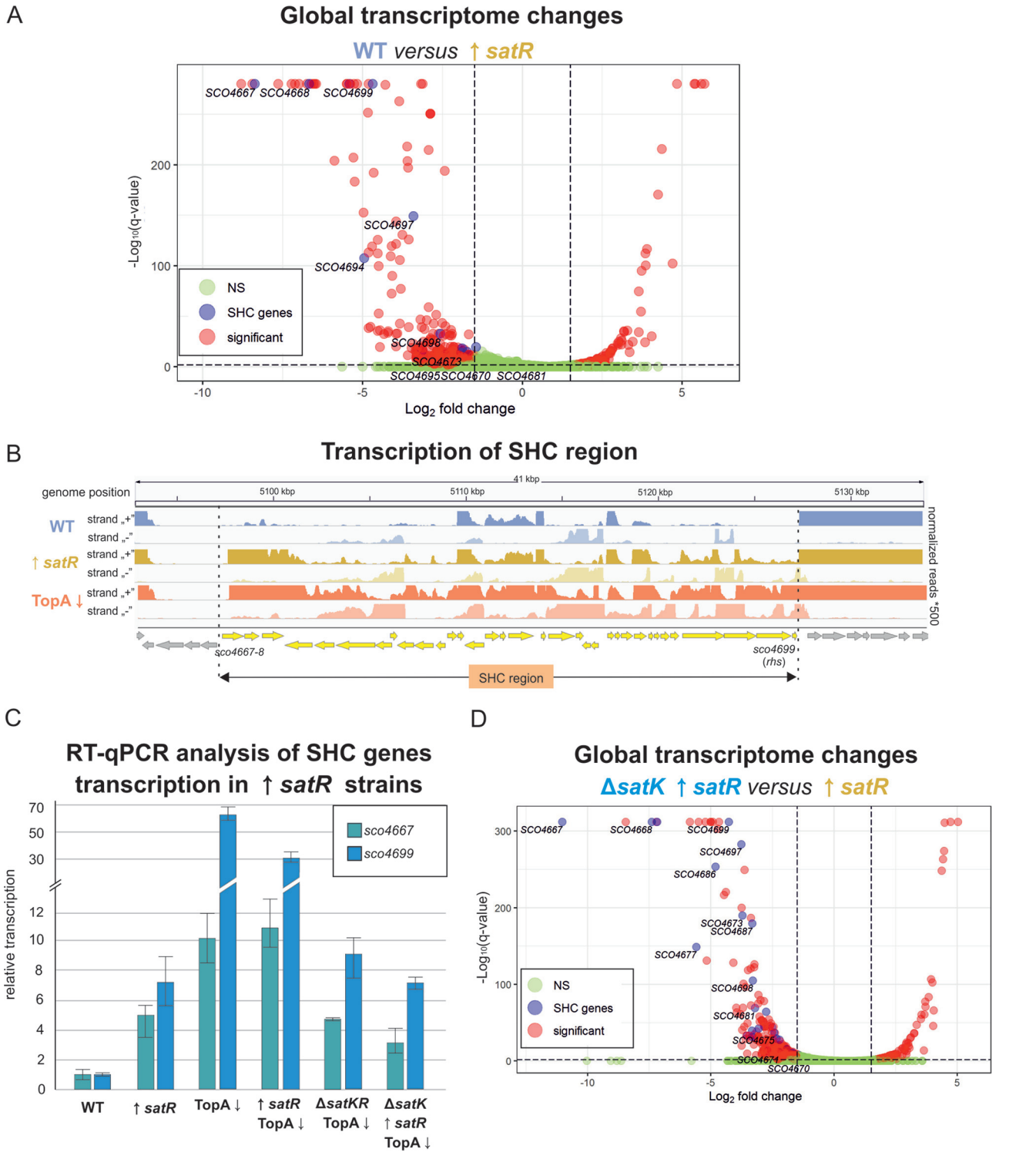

FIG 5 Global transcriptome analysis of strains overexpressing *satR* in the presence of SatK (MGM11) and in the *satK* background (MGM14). (A) Volcano plot based on RNA-seq experiments showing changes in global gene expression between the wild-type (WT) and *satR*-overexpressing strain MGM11 (*satR*↑). Significantly altered transcripts ($q \leq 0.01$ and $1.5 < \log_2$ fold < -1.5) are depicted in red, SHC genes are shown in blue, and nonsignificant (NS) changes are marked in green. (B) Transcriptional profile of the SHC region in the MGM11 strain overexpressing *satR* (*satR*↑; yellow) compared with its wild-type parental strain (WT; blue) and TopA-depleted PS04 strain (TopA↓; orange). (C) RT-qPCR analysis of *sco4667* and *sco4699* gene transcription levels in the WT, TopA-depleted PS04 strain (TopA↓), TopA-depleted MGP12 strain carrying a deletion of *satKR* (Δ*satKR* TopA↓), MGM11 strain overexpressing *satR* in the wild-type background (*satR*↑), MGP11 strain overexpressing *satR* in the TopA-depleted background (*satR*↑ TopA↓), and MGP14 strain overexpressing *satR* in the TopA-depleted *satK* deletion (*satR*↑ Δ*satK* TopA↓) background. (D) Volcano plot based on RNA-seq experiments showing changes in global gene expression between strain MGM14 overexpressing *satR* in the absence of SatK (*satR*↑ Δ*satK*) and strain MGM11 overexpressing SatR in the wild-type background (*satR*↑). Significantly altered transcripts ($q \leq 0.01$ and $1.5 < \log_2$ fold < -1.5) are depicted in red, SHC genes are shown in blue, and nonsignificant changes are marked in green.

genes, including SHC even under normal supercoiling conditions, its overexpression in the absence of kinase resulted in much less pronounced changes in transcription both in the wild-type and increased supercoiling backgrounds (MGM14 and MGP14, respectively) (Data Set S1, Tab 7 and Tab 8). In conditions of normal supercoiling, overexpression of *satR* in a *satK* mutant background led to transcriptional activation of only 15 genes and repression of 17 genes compared with the wild type. Similarly, overexpressing *satR* in the *satK* mutant, TopA-depleted background led to changes in the expression of 19 genes (14 activated and 5 repressed) compared with the TopA-depleted strain. Furthermore, when comparing the effect of *satR* overexpression in the wild-type and *satK* deletion backgrounds (MGP11 and MGP14, respectively), we found that all SHC genes activated by *satR* overexpression in the presence of SatK were silenced when the kinase was absent (Fig. 5D, confirmed by RT-qPCR [Fig. 5C]). This evidence strongly suggested that SatK-phosphorylated SatR functions to activate—either directly or indirectly—the SHC genes.

In summary, we confirmed that the SatKR system contributed to the activation of SHC gene transcription. The results of our transcriptional analyses suggest that SatR functions predominantly as a transcriptional activator, and its activity requires the presence of SatK. Interestingly, our data suggested that both SatKR and supercoiling were sufficient to independently activate SHC transcription. Moreover, the activation of SHC genes either by supercoiling or SatR activity was correlated with slower growth and sporulation inhibition.

A single transposon insertion in the SHC induces sporulation under TopA depletion. Our findings suggested that increased SHC expression may be contributing to sporulation defects, given the reduced sporulation observed in both a TopA-depleted strain (high supercoiling, high SHC expression) and an *satR* overexpression strain (high SHC expression). Consistent with this possibility was our finding that one of our original transposon mutant strains that restored sporulation to a TopA-depleted strain had an insertion in the penultimate SHC gene *sco4699* (strain MGHM14). *sco4699* encodes a homologue of the Rhs protein from *E. coli*, a secreted toxin that mediates cellular competition (43). In this mutant strain, the *Himar1* transposon was inserted 311 nucleotides downstream of the *sco4699* start codon (Fig. 6A).

As was seen for the *satKR*-associated transposon mutant, the growth rate of the TopA-depleted MGHM14 strain (where TopA depletion was confirmed by Western blot analysis [Fig. S7]) was partially restored, both on solid medium and in liquid medium, compared with its TopA-depleted parental strain (Fig. 6B and C). We observed abundant spore chains in the TopA-depleted SHC transposon mutant, while in its parental TopA-depleted strain (PS04), no spore chains could be detected (Fig. 6B). Moreover, similar to what was observed when *satKR* was disrupted by transposon insertion (in the MGHM5 strain), transposon integration into *sco4699* also resulted in formation of spores of varied sizes (Fig. 6D).

Since *sco4699* product supposedly does not act as transcriptional regulator, we wondered whether the supercoiling-dependent transcriptional regulation of the SHC region might be modified by transposon insertion in *sco4699*, providing a rationale for the restored sporulation. Thus, we used RT-qPCR to test the transcription level of the first SHC gene (*sco4667*) in this mutant background. We found that transposon insertion in *sco4699* silenced expression of the cluster even when TopA was depleted (Fig. 6E), similarly to what had been observed for the *satKR* mutant.

Next, to confirm that the downregulation of the first gene of the SHC resulted from transposon insertion in the last gene of the cluster, we reconstructed the SHC transposon strain by inserting a hygromycin resistance cassette in *sco4699* (at the transposon insertion site) in the TopA-controlled background (MGP20 strain). RT-qPCR analysis confirmed that transcription of the first gene within the SHC region (*sco4667*) was silenced in the TopA-depleted strain (Fig. 6E). This analysis suggested that supercoiling-dependent activation of the SHC genes might be disrupted by insertion in a distant region of the gene cluster.

In summary, the mutation of *sco4699* within the SHC region inhibited cluster

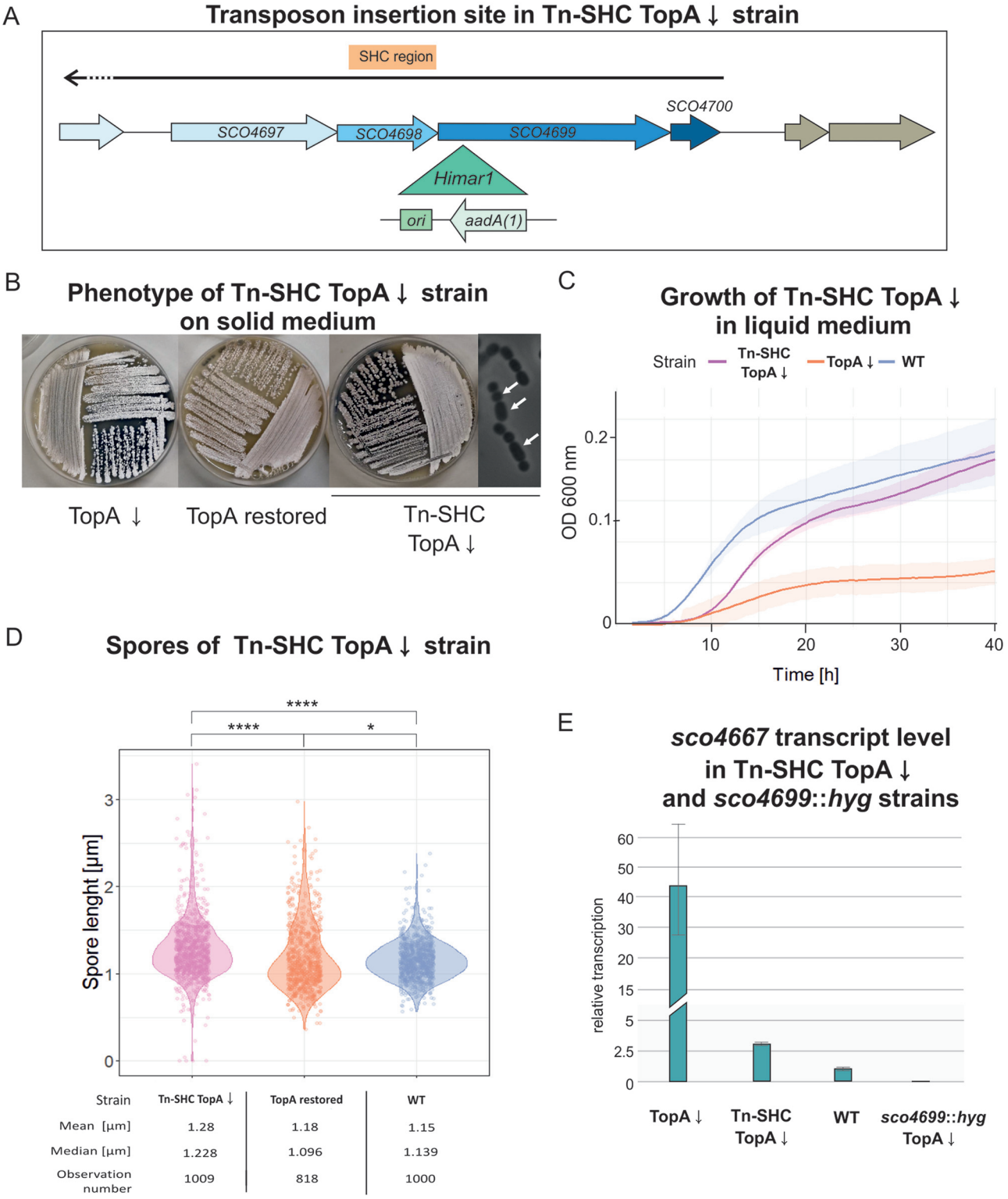

FIG 6 Phenotype of the SHC transposon strain MGHM14. (A) *Himar1* transposon insertion site of the transposon in MGHM14 (Tn-SHC). The green triangle shows the insertion site with the orientation of the inserted *aadA(1)* gene. (B) Growth and differentiation of the TopA-depleted transposon MGHM14 (Tn-SHC TopA↓) compared with the wild-type (WT) and TopA-depleted PS04 strain (TopA↓) on MS agar after 72 h of growth. (C) Growth curve of TopA-depleted MGHM14 (Tn-SHC TopA↓) compared with the wild-type (WT) and TopA-depleted strain PS04 (TopA↓) in liquid 79 broth obtained using a Bioscreen C instrument. Measurements were performed in triplicate every 20 min for 42 h. (D) Spore size distribution in the TopA-depleted MGHM14 strain (Tn-SHC TopA↓), its parental strain PS04 with TopA levels restored by induction with 1 μg/ml thiostrepton (TopA restored) and the wild-type (WT) strain. Asterisks indicate the significance of the *P* value (*, $P \leq 0.05$; ****, $P \leq 0.0001$) when comparing mean spore sizes. (E) RT-qPCR analysis of *sco4667* transcription in TopA-depleted MGHM14 (Tn-SHC TopA↓) and TopA-depleted *sco4699* mutant strains (*sco4699::hyg* TopA↓) compared with the wild-type (WT) and TopA-depleted PS04 strains (TopA↓).

activation by supercoiling. Moreover, mutations in *sco4699* reinforced the idea that silencing of the SHC under conditions of high supercoiling restores sporulation.

Deletion of SHC genes (*sco4667-4668*) encoding a two-component system SitKR restores sporulation in conditions of high supercoiling. To further probe the contribution of the SHC genes to the inhibition of sporulation under conditions of high chromosome supercoiling, we sought to test whether specific genes within the SHC region might be responsible. As the first gene of the SHC region (*sco4667*) was annotated as encoding a kinase of another putative two-component system and formed the operon with the *sco4668* gene, encoding its cognate response regulator, we deleted *sco4667-4668* together in the wild-type and TopA-controlled backgrounds (MB01 and MB02 strains, respectively).

We found that the *sco4667-4668* deletion—like the *satK* transposon insertion and mutation of *sco4699*—partially restored the growth of the TopA-depleted strain in liquid cultures compared with its TopA-depleted parental strain, while having no effect on growth in the wild-type background (Fig. 7A). Sporulation of the *sco4667-4668* mutant strain in the TopA-depleted background was also restored; this was confirmed microscopically but was observed only after prolonged incubation (120 h of growth on MS agar) (Fig. 7B). As before, spores of the TopA-depleted *sco4667-4668* mutant also exhibited a diversity in size, with a greater mean length than that of the wild type (Fig. 7C). Given the ability of this novel two-component system encoded within the SHC to influence growth and sporulation under conditions of high supercoiling, it was named SitKR (sporulation-inhibiting two-component system kinase and regulator).

Since we found that insertion in the second to last SHC gene abolished TopA depletion-dependent activation of the first SHC gene *sco4667*, we tested whether *sitKR* deletion affected transcription of the penultimate SHC gene. RT-qPCR analysis confirmed that the deletion of *sitKR* genes caused a downregulation of *sco4699* under high supercoiling conditions (Fig. 7D).

This analysis reinforced the idea that mutations of genes within the SHC region can have profound effects on the supercoiling-dependent transcription of more distant genes. Moreover, these results further support the notion that inhibition of SHC gene induction under elevated supercoiling conditions restores the sporulation of TopA-depleted strains. Finally, we have shown that a second two-component system, SitKR, inhibits sporulation when transcriptionally induced by SatKR.

DISCUSSION

TopA depletion in *Streptomyces* inhibits growth and sporulation. Before, we showed that *parB* deletion in the TopA-depleted strain partially suppresses the white phenotype and restores spore formation in *S. coelicolor* (38). This indicated that topological tension generated during formation of ParB complexes could inhibit their segregation and impair progress of sporulation at TopA depletion (38). However, we expected that additional explanation of the white phenotype of TopA-depleted mutant could be supercoiling-induced changes in the transcription of unknown sporulation/growth regulators. The application of random transposon mutagenesis in the TopA-depleted *S. coelicolor* strain allowed us to identify novel proteins engaged in sporulation regulation. Among the newly identified sporulation regulators was a two-component system named SatKR conserved in *Streptomyces*. The SatKR regulon includes a supercoiling-hypersensitive cluster that is also independently activated by TopA depletion. Transposon insertion in the *satK* gene encoding the kinase led to lower levels of SatR and was observed to revert the TopA depletion-induced activation of SHC and restored growth and sporulation. In contrast, increased SatR levels in the presence of its cognate kinase at wild-type supercoiling levels led to the activation of transcription of numerous SHC genes, inhibiting *Streptomyces* development.

The two-component system SatKR controls growth and differentiation by regulating SHC genes. *Streptomyces* two-component systems are known to control antibiotic production, central metabolism, morphology, and differentiation (36). Although numerous TCSs in *Streptomyces* affecting these processes have been well described (e.g., CepRS [44], MacRS [45], PhoRP [46, 47], OsdKR [48], AfsQ1/Q2 [49], and DraRK [50]), the

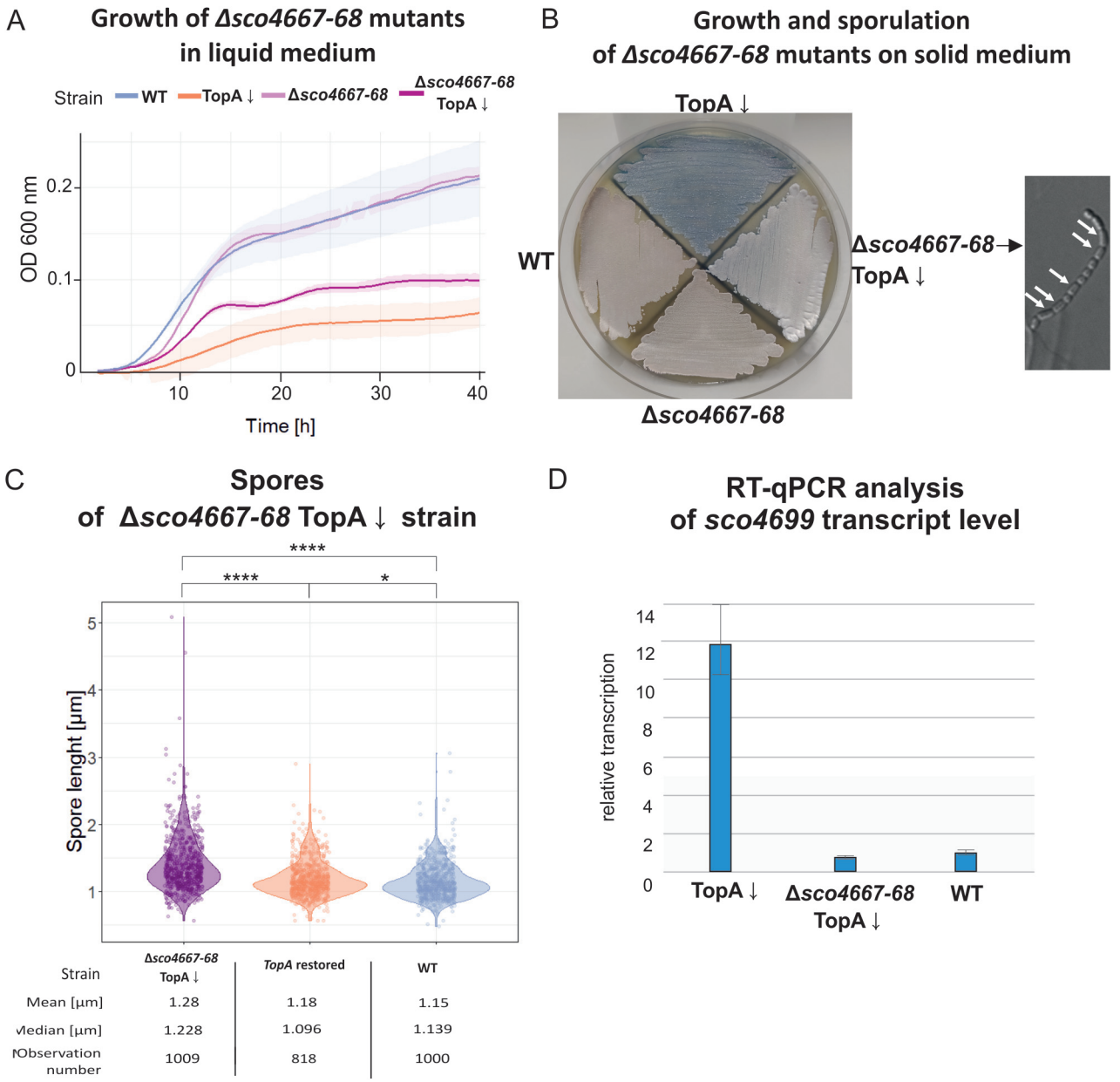

FIG 7 Phenotype of Δ*sco4667-4668* mutants in wild-type (MB01) and TopA-depleted backgrounds (MB02). (A) Growth curves of MB01 (Δ*sco4667-4668*) and the TopA-depleted MB02 strain (Δ*sco4667-4668* TopA↓) compared with the wild-type (WT) and TopA-depleted strain PS04 (TopA↓) in liquid 79 broth obtained using a Bioscreen C instrument. Measurements were performed every 20 min for 42 h. (B) Growth and differentiation of the MB01 (Δ*sco4667-4668*) and TopA-depleted MB02 (Δ*sco4667-4668* TopA↓) strains, respectively, compared with the wild-type (WT) and TopA-depleted strain PS04 (TopA↓) after 120 h of growth on MS agar. A microscopic image of the spore chain of the TopA MB02 strain (Δ*sco4667-4668* TopA↓) after 48 h of growth in MM minimal medium (with 1% mannitol) is shown to the right of panel B. (C) Spore size distribution in TopA-depleted MB02 (Δ*sco4667-4668* TopA↓) compared with the parental PS04 strain with restored TopA levels induced with 1 μg/ml thiostrepton (TopA restored) and with wild type (WT). Asterisks indicate the significance of the *P* value (*, $P \leq 0.05$; ****, $P \leq 0.0001$) when comparing mean spore sizes. (D) RT-qPCR analysis of the transcription of *sco4699* located at the end of the SHC region in the TopA-depleted MB02 strain (Δ*sco4667-4668* TopA↓) compared with the TopA-depleted PS04 (TopA↓) and wild-type (WT) strain. RNA was isolated from a 24-h culture in liquid 79 broth.

identification of signals to which TCSs respond has been successful for only a few TCSs (e.g., phosphate concentrations for PhoPR [46], nitrogen concentrations for AfsQ1/Q2 [49] and DraRK [50], iron availability for AbrA1/A2 [51], and redox stress for SenSR [52]). Here, we have established a role for SatKR in regulating growth rate, differentiation, and antibiotic production in *S. coelicolor*, but we were unable to predict the SatKR activation signal on the basis of our data. It should be noted that *satKR* gene expression is unresponsive to

changes of DNA supercoiling; however, this does not exclude a signal related to changes of DNA topology.

Our results suggested that both the SatR levels in the cell and its activation by the cognate kinase SatK influenced the growth and development of *S. coelicolor*. SatR is a sequence homologue of the DegU response regulator from the *Bacillus subtilis* DegUS two-component system (37.2% identity with 223 amino acids [aa] of overlap). In *B. subtilis*, DegU controls flagellum synthesis, antibiotic production, and biofilm formation, inducing the expression of genes involved in matrix formation, competition, and nutrient acquisition (53). Interestingly, the *S. coelicolor* genome encodes another DegUS homologue, SCO5784-5785, with a similar percentage identity to DegUS proteins as SatKR. Moreover, SCO5784-5785 has also been shown to influence sporulation as well as antibiotic production; however, its effect on *Streptomyces* differentiation seems to be opposite that of SatKR (54). Markedly, some DegU-regulated genes are induced independently of its phosphorylation (55). Given that SatR stimulates SHC transcription only in the presence of a functional cognate kinase SatK and that reduced levels of SatR in the absence of SatK (in the transposon mutant) lead to the inhibition of SHC transcription despite high DNA supercoiling conditions, we inferred that both SatR states (phosphorylated and unphosphorylated [see below]) were able to regulate transcription, although with different effects on the regulated genes. An interesting feature is a localization of the *sco3388* gene downstream of the *satKR* genes, presumably forming an operon. *sco3388* is similar to the *trmB* gene from *B. subtilis*; however, it was previously shown that, in contrast to its homolog, *sco3388* does not determine tunicamycin resistance (56). SCO3388 was indicated to control cell wall integrity and influence spore viability (56); thus, its proximity to *satKR* genes may suggest their cooperation in controlling sporulation in *S. coelicolor*.

Since the SatR regulon includes the SHC cluster and SHC is induced in the TopA-depleted strain (12), we concluded that the activation of one or more of the 26 supercoiling-sensitive SHC genes may be responsible for the growth and sporulation inhibition. The SHC region is unique to *S. coelicolor* and shows low synteny among *Streptomyces*, even though homologues of individual SHC genes can be found in other species (see Fig. S8 and Data Set S1, Tab 9, in the supplemental material). The functions of many of the SHC genes remain unknown, but those genes with predicted functions encode two-component systems (*sco4667-4668*), two probable regulators (*sco4671* and *sco4673*), a putative Rhs protein (*sco4699*), and the RsfA anti-sigma factor (*sco4677*) (57) that represses SigF, a sporulation-specific sigma factor (58, 59).

The first SHC operon, *sco4667-4668*, encoded another novel two-component system named SitKR, which seems to be critical for sporulation and growth. SitKR is conserved among *Streptomyces* species; however, its chromosomal location differs among species. Interestingly, the regulation of *sitKR* gene expression by SatKR is a phenomenon of a two-component system signaling cascade that has been observed for only a few bacterial species, e.g., SsrAB regulation by OmpR/EnvZ and PmrAB by PhoPQ in *S. enterica* (60, 61) and RseDE regulation by PhoPR in *B. subtilis* (62). *sitKR* genes are among the most significantly induced by TopA depletion and *satR* overexpression. Whereas deletion of *satKR* did not restore sporulation in the TopA-depleted strain, a strain in which the *sitKR* genes had been deleted was capable of producing spores. The regulon of *sitKR* has not been established; however, we found that operon deletion abolished supercoiling induction of other genes in the SHC (e.g., *sco4699*). While SitR may directly control the expression of *sco4699* (and possibly other SHC genes), there may also be synchronized regulation between (at least) the first (*sitKR*) and last genes (*sco4699-4700)* within the SHC region. We cannot exclude the possibility that upregulation of *sco4677* (encoding anti-sigF) by SatR (and possibly by SitKR) or by increased DNA supercoiling can significantly contribute to sporulation inhibition.

The significance of SHC gene induction for the inhibition of growth and sporulation of the TopA-depleted strain was reinforced by the identification of transposon mutations in the next to the last gene of the SHC region (*sco4699*), which led to restored

sporulation in the TopA-depleted strain. *sco4699* encodes a homologue of the Rhs protein from *E. coli*, where Rhs is a secreted toxin that mediates cellular competition (43). Importantly, transposon insertion in *sco4699* also abolished the expression of the first SHC gene, *sitK*. It is possible that the observed effect on sporulation and growth in the SHC transposon strain was due to Rhs inactivation, but we consider the abolished induction of *sitKR* by TopA depletion to be a more likely explanation for the restored sporulation in the transposon strain.

Thus, abolished induction of the SHC region upon TopA depletion in three distinct mutant strains (transposon in *satK*, transposon in *rhs*, and deletion of *sitKR*) restored growth and sporulation despite lowered TopA levels and high chromosomal supercoiling. Notably, spores produced by all the strains with high DNA supercoiling and inhibited SHC transcription had varied sizes and impaired resistance to damaging agents. This phenomenon could result from a lack of additional factors that are needed for proper spore formation and maturation, which may be encoded outside the SHC region. Nevertheless, we established that genes within the SHC region were under the control of the SatKR two-component system and included sporulation and growth rate inhibitors. We speculate that in response to unidentified factors, SatKR induces SHC genes to support slower growth and inhibit sporulation under unfavorable, possibly DNA topology-affecting conditions. Given that a similar induction of SHC genes results from increased supercoiling, we hypothesize that both factors, i.e., changes in chromosome supercoiling and SatKR activation, would independently prevent sporulation under specific environmental conditions, possibly connected with chromosome damage.

The two-component system SatKR collaborates with chromosome supercoiling in the regulation of gene expression. SHC genes are subject to no or low transcription in the wild-type *S. coelicolor* strain under standard culture conditions, but they are activated by high DNA supercoiling as a result of TopA depletion. However, the presumed low levels of SatR resulting from kinase inactivation (transposon mutant, with low *satR* transcript levels) completely abolished SHC induction by high DNA supercoiling. Importantly, the deletion of *satKR* genes together did not abolish SHC activation by increased DNA supercoiling. Thus, we suggest that in addition to the presence of the kinase, the SatR phosphorylation state may also depend on SatR protein level. Taking into account the possibility of nonspecific activation of SatR by other cellular factors (e.g., acetyl phosphate [AcP] [63] or noncognate TCS kinases [64]), we suggest that SatR overproduction results in inefficient or nonspecific modification of SatR. Additionally, considering the potential phosphatase activity associated with many kinases, at this stage we cannot predict the phosphorylation state of SatR in the presence and absence of SatK; however, we assume that it is different in those two genetic backgrounds. Since we established that deletion of *satKR* genes had different effects on growth and gene expression than a transposon inserted in *satK*, we speculate that upon *satK* inactivation, SatR in its inactive state may also bind to DNA and control the expression of SHC genes, reversing their activation by high supercoiling. This could be achieved either by different DNA binding specificities/affinities for phosphorylated and unphosphorylated SatR or different abilities to form higher-order complexes or interact with RNA polymerase. Our speculation here is supported by evidence showing that other two-component system response regulators can act when unphosphorylated (65), e.g., OmpR (66, 67), PhoP (68), SsrB (69), and DegU (55).

Possible explanations for the coordinated regulation of gene transcription by DNA supercoiling and transcription factor activity could include the formation of a supercoiled DNA loop due to transcription factor binding, or supercoiling-dependent binding of transcription factors. Synchronized activation of the SHC region could suggest formation of the loop encompassing this region, stabilized by SatR. Moreover, loop formation could depend on global DNA supercoiling. There is published evidence for DNA looping by some repressor proteins promoted by supercoiling, e.g., LacI in *E. coli* or bacteriophage λ (70, 71), because DNA compaction increases the likelihood of bringing together distant binding sites. Therefore, the affinity of SatR for DNA could be altered not only by its phosphorylation but also by DNA supercoiling. Indeed, the

binding of some response regulators has been shown to be influenced by DNA supercoiling, e.g., OmpR binding in *S. enterica* (72).

Elevated *satR* transcription in the presence of kinase activated SHC transcription in the wild-type strain, showing that the SatKR system could control the SHC region independently of DNA supercoiling. In other bacterial species, it has also been suggested that two-component systems might influence the DNA supercoiling state by interacting with topoisomerases or altering their activity. In *Staphylococcus aureus*, deletion of the ArlSR two-component system elevates DNA supercoiling (73), while the *E. coli* RstB response regulator interacts with TopA and increases its activity (74). Although we observed elevated supercoiling in the TopA-depleted strain with a transposon insertion in *satK*, and lowered *satR* transcript levels, we cannot exclude the possibility that local DNA topology changes when SatR binds.

We propose a model in which SatR and DNA supercoiling (caused by TopA depletion), both independently and cooperatively, regulate SHC transcription (Fig. 8). SatR, as a two-component system regulator in the presence of SatK kinase, activates SHC transcription. However, in the absence of kinase, SatR also regulates the transcription of SHC genes, reversing their activation by high supercoiling. Induction of SitKR, an SHC-encoded two-component system, inhibits sporulation; however, it is still unclear whether this sporulation defect is a direct effect or whether other SHC-encoded proteins are involved. Our results are indicating that there is an unprecedented complex regulatory interplay that connects DNA supercoiling with a cascade of two-component regulatory systems in controlling growth and sporulation in *Streptomyces*.

MATERIALS AND METHODS

Bacterial strains, plasmids, and growth conditions. Basic DNA manipulations were performed according to standard protocols (75). Unless otherwise stated, all enzymes and isolation kits were supplied by Thermo Fisher Scientific (Waltham, MA, USA) and New England Biolabs (Ipswitch, MA, USA). Bacterial media and antibiotics were purchased from Difco Laboratories (Detroit, MI, USA) and Carl Roth (Karlsruhe, Germany), respectively. The *S. coelicolor* strains used in this study are listed in Text S1A in the supplemental material. Strain construction details are provided in Text S1B. The growth conditions, antibiotic concentrations, and *S. coelicolor* conjugation procedure as described by Kieser et al. (76) were used. To restore TopA levels in the TopA-controlled strain (PS04) (during growth analysis and spore sensitivity assay), the growth medium was supplemented with 0.5 to 1 μg/ml thiostrepton (77). During conjugation with the PS04 strain, thiostrepton concentrations of 5 μg/ml were used, unless otherwise stated (it was earlier shown that induction with thiostrepton at a concentration higher than 2 μg/ml increases TopA levels only slightly above the level of the wild type).

For growth rate analyses, *S. coelicolor* cultures were inoculated with spores diluted to an optical density at 600 nm (OD_{600}) of 0.01/ml in 79 medium (peptone 1% v/o, casein hydrolysate 0.2% v/o, yeast extract 0.2%, NaCl 0.1 M, pH 7.2 to 7.4). To determine the growth rate, cultures were grown for 48 to 55 h in microplates in a final volume of 300 μl using a Bioscreen C instrument (Oy Growth Curves Ab Ltd., Helsinki, Finland), with optical density (OD_{600}) measurements being taken at 20-min intervals. To analyze *S. coelicolor* differentiation, strains were plated on solid MS agar medium (76) and cultured for 3 to 7 days.

Transposon mutagenesis. Random transposon mutagenesis was performed on the TopA-controlled strain (PS04) using the synthetic *Himar1* transposon (3,276 bp in length, containing a spectinomycin resistance gene [*aadA(1)* and R6Kγ *ori* flanked with ITRs (inverted terminal repeats)] (78). Exconjugants were selected using hygromycin and spectinomycin, in addition to 0.2 μg/ml thiostrepton, to limit transposase induction but increase the TopA level. Spores of exconjugants were collected and inoculated into liquid cultures with thiostrepton (0.2 μg/ml); these were cultivated at 39°C overnight to eliminate the pHSM plasmid. The mutant library was then spread for single colonies (to obtain at least 16,000 mutants) on MS agar plates supplemented with spectinomycin but no thiostrepton (the PS04 strain has a "white phenotype" under these conditions), and gray colonies were screened for. The transposon insertion sites in the selected transposon library clones were identified using a rescue plasmid approach (78). In the MGHM5 strain (PS04 *sco3390*::*Himar1 sco2474*::*Himar1*), insertion sites were additionally confirmed by whole-genome sequencing (Genomed, Warsaw, Poland).

Supercoiling reporter plasmid isolation. The pWHM3Hyg/pWHM3Spec plasmid, which served as a probe of the DNA supercoiling state *in vivo*, was isolated according to a previously described procedure (77) from *S. coelicolor* strains (MGHM5_RP, MS10, and MS11—derivatives of analyzed mutants modified by pWHM3Hyg introduction), where these strains were cultivated in liquid 79 medium for 24 h at 30°C. The isolated plasmid DNA was resolved on a 0.8% agarose gel with 2.32 μg/ml chloroquine in Tris-acetate-EDTA (TAE) buffer. To visualize topoisomers, the gel was stained with ethidium bromide. The topoisomer distribution was analyzed using ImageJ Software.

RNA-Seq and data analysis. For the RNA-seq experiments, RNA was isolated from *S. coelicolor* mycelia obtained from 18-h cultures in 30 ml YEME/tryptic soy broth (TSB) liquid medium (76). The mycelia were collected by centrifugation, frozen, and stored at −70°C for subsequent RNA isolation.

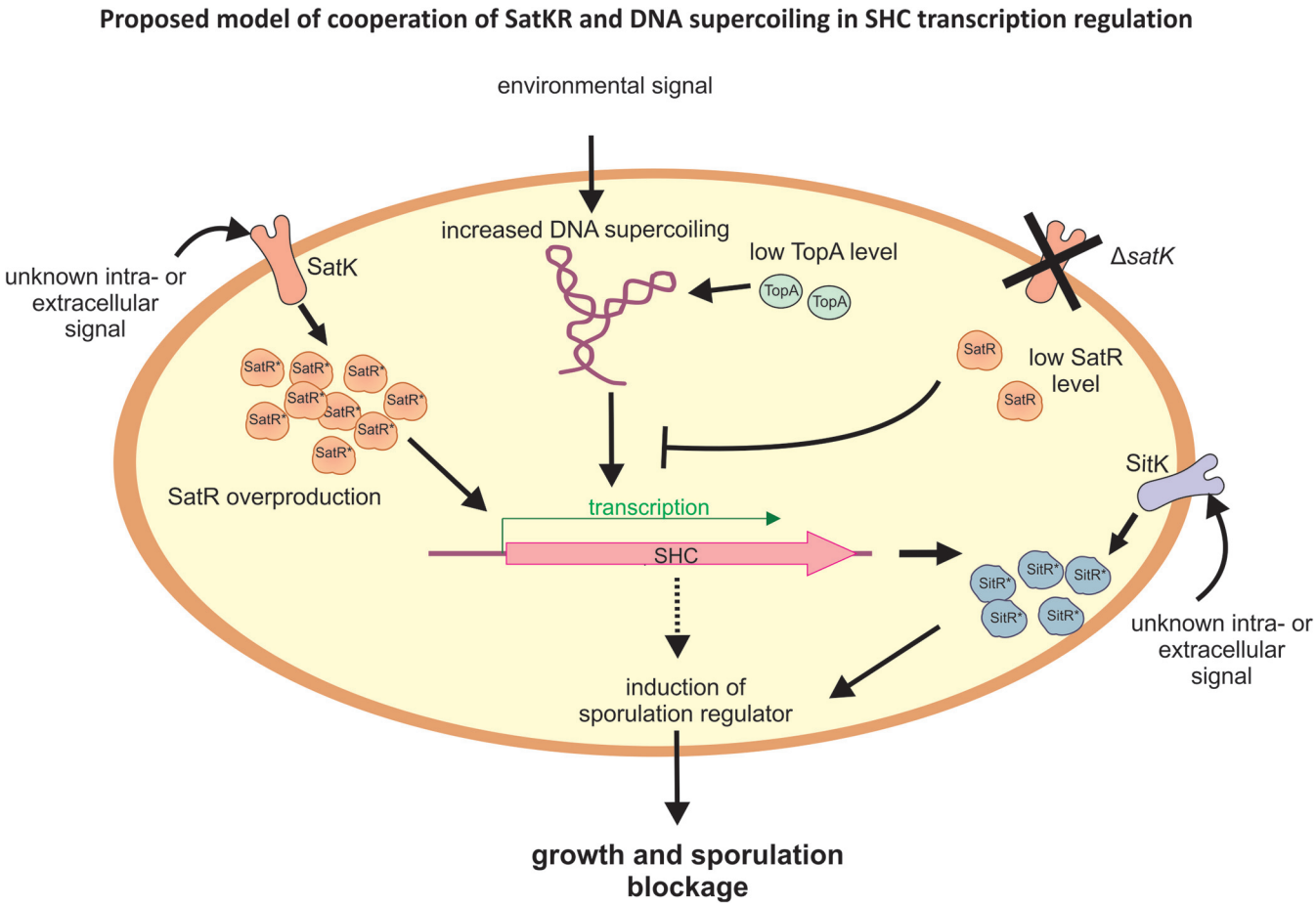

FIG 8 Proposed model of cooperation of SatKR, SitKR, and DNA supercoiling in SHC transcription regulation and sporulation inhibition. SHC genes are activated by elevated DNA supercoiling. In the absence of SatK and at low level, SatR inhibits supercoiling-dependent activation of SHC transcription. At high intracellular concentration and when activated by the cognate kinase SatK, SatR induces transcription of SHC genes, independently of supercoiling. Among SHC products is SitKR two-component system, which is involved in sporulation inhibition. Contribution of other SHC gene-encoded proteins in the sporulation inhibition is also probable.

RNA was isolated using the procedure described previously by Moody et al. (84), after which the preparations were subjected to digestion with TURBO DNase I (Invitrogen, Waltham, MA, USA) and checked using PCR to ensure the samples were free of chromosomal DNA contamination. Strand-specific cDNA libraries with an average fragment size of 250 bp were constructed and sequenced using a MiSeq kit (Illumina, San Diego, CA, USA) at the Farncombe Metagenomics Facility at McMaster University (Hamilton, Canada). Paired-end 76-bp reads were subsequently mapped against the *S. coelicolor* chromosome using Rockhopper software (79), achieving 1.0×10^6 to 1.5×10^6 successfully aligned reads per sample. For data visualization, Integrated Genomics Viewer (IGV) software was used (80, 81). The analysis of differentially regulated genes was based on the data generated by Rockhopper software. To calculate the fold change in gene transcription, the normalized gene expression in the control strain (wild type [WT] or PS04) was divided by the normalized gene expression under particular experimental conditions, delivering information on the fold change, and subsequently, the $\log_2$ value of the fold change was calculated. The genes with a *q* value (Rockhopper adjusted *P* value) greater than or equal to 0.01 and a $\log_2$ fold change in the range from −1.5 to 1.5 were rejected from the subsequent analysis as not significant. Volcano plots were prepared using R Studio software and the EnhancedVolcano package (R package version 1.10.0; https://github.com/kevinblighe/EnhancedVolcano).

RT-qPCR. For RT-qPCR analyses, RNA was isolated from *S. coelicolor* mycelia obtained from 24-h cultures growing in 5 ml of liquid 79 medium. Transcription was arrested by adding STOP solution (95% ethanol [EtOH] [vol/vol], 5% phenol [vol/vol]) (82), and mycelia were harvested by centrifugation and frozen at −80°C. Total RNA was isolated using TRI-Reagent (Sigma-Aldrich, Saint Louis, MO, USA) according to the manufacturer's procedure. Homogenization was performed in a FastPrep-24 instrument (MP Biomedicals, Irvine, CA, USA) (6 m/s, 2 cycles × 45 s). After centrifugation, RNA was isolated by chloroform extraction, purified on a column (Total Mini RNA, AA Biotechnology, Gdańsk, Poland), and eluted with 50 μl of ultrapure water. The isolated RNA was digested with TURBO DNase (Invitrogen) according to the manufacturer's instructions at 37°C for 30 min. Then, RNA was purified and concentrated using a CleanUp RNA Concentrator (AA Biotechnology) and eluted with 17 μl of ultrapure water. Five hundred

nanograms of RNA was used for cDNA synthesis using a Maxima First Strand cDNA synthesis kit (Thermo Fisher Scientific) in a final volume of 20 μl. The original manufacturer's protocol was modified for GC-rich transcripts by increasing the temperature of the first-strand synthesis to 65°C and elongation time up to 30 min. Subsequently, the obtained cDNA was diluted five times and used directly for quantitative PCRs performed with PowerUp SYBR green Master Mix (Applied Biosystems, Waltham, MA, USA). The relative level of a particular transcript was quantified using the comparative $\Delta\Delta C_T$ method, and the *hrdB* gene was used as the endogenous control (StepOne Plus real-time PCR system; Applied Biosystems). The sequences of optimized oligonucleotides used in this study are given in Text S1C.

Microscopic analyses. For analysis of spore formation, the tested strains were inoculated at the acute-angled junctions of coverslips inserted at 45° into minimal medium agar plates supplemented with 1% mannitol and cultured for 53 h to ensure sporulation of all mutant strains. Sporulation of the TopA-controlled (PS04) strain was induced by the addition of 1 μg/ml thiostrepton. Coverslips were fixed with methanol and then mounted using 50% glycerol solution in phosphate-buffered saline (PBS). DNA was stained with a 2-μg/ml 4′,6′-diamidino-2-phenylindole (DAPI) solution (Molecular Probes, Eugene, OR, USA). Microscopic analyses were performed using a Leica microscope (Leica Microsystems, Wetzlar, Germany) with phase-contrast imaging. Images were analyzed using ImageJ software. The statistical analysis of spore length was performed using RStudio (83) and the Student's *t* test for paired samples.

Spore sensitivity assay. To test spore viability, *S. coelicolor* strains were cultured on MS agar plates for 5 days. Next, the spores were collected and incubated in 5% SDS (sodium dodecyl sulfate) solution for 1.5 h, washed twice with ultrapure water, and resuspended in 0.5 ml of water. Next, serial dilutions were spread on MS agar plates to obtain single colonies. Subsequently, the number of colonies grown after SDS treatment was compared with the negative control (spores of the same strain collected and incubated in water). Spore viability was calculated as a ratio of the number of colonies obtained for spores treated and untreated with SDS.

Data availability. RNA-seq data are available at ArrayExpress (EMBL-EBI) accession number E-MTAB-10835.

SUPPLEMENTAL MATERIAL

Supplemental material is available online only.

DATA SET S1, XLSX file, 0.1 MB.

TEXT S1, PDF file, 0.6 MB.

FIG S1, JPG file, 2 MB.

FIG S2, JPG file, 2.5 MB.

FIG S3, JPG file, 2.2 MB.

FIG S4, JPG file, 2.1 MB.

FIG S5, JPG file, 2.3 MB.

FIG S6, JPG file, 1.9 MB.

FIG S7, JPG file, 1.8 MB.

FIG S8, JPG file, 2.2 MB.

ACKNOWLEDGMENTS

We thank Govind Chandra (John Innes Centre, Norwich, UK) for the bioinformatics analysis of SHC gene synteny among *Streptomyces*.

This work was supported by the Polish National Science Centre (OPUS grant 2014/15/B/NZ2/01067 to D.J.); Natural Sciences and Engineering Research Council of Canada (Discovery grant RGPIN-2020-07197 to M.A.E.) and Canadian Institutes of Health Research (project grant PJT-162340 to M.A.E.). Publication was financed by the program "Initiative of Excellence – Research University."

REFERENCES

1. Browning DF, Busby SJW. 2016. Local and global regulation of transcription initiation in bacteria. Nat Rev Microbiol 14:638–650. https://doi.org/10.1038/nrmicro.2016.103.
2. Lloyd G, Landini P, Busby S. 2001. Activation and repression of transcription initiation in bacteria. Essays Biochem 37:17–31. https://doi.org/10.1042/bse0370017.
3. Dorman CJ, Dorman MJ. 2016. DNA supercoiling is a fundamental regulatory principle in the control of bacterial gene expression. Biophys Rev 8:209–220. https://doi.org/10.1007/s12551-016-0205-y.
4. Groisman EA. 2016. Feedback control of two-component regulatory systems. Annu Rev Microbiol 70:103–124. https://doi.org/10.1146/annurev-micro-102215-095331.
5. Zschiedrich CP, Keidel V, Szurmant H. 2016. Molecular mechanisms of two-component signal transduction. J Mol Biol 428:3752–3775. https://doi.org/10.1016/j.jmb.2016.08.003.
6. Champoux JJ. 2001. DNA topoisomerases: structure, function, and mechanism. Annu Rev Biochem 70:369–413. https://doi.org/10.1146/annurev.biochem.70.1.369.
7. Dorman CJ, Corcoran CP. 2009. Bacterial DNA topology and infectious disease. Nucleic Acids Res 37:672–678. https://doi.org/10.1093/nar/gkn996.
8. Ferrándiz M-J, Martín-Galiano AJ, Arnanz C, Camacho-Soguero I, Tirado-Vélez J-M, de la Campa AG. 2016. An increase in negative supercoiling in bacteria reveals topology-reacting gene clusters and a homeostatic response mediated by the DNA topoisomerase I gene. Nucleic Acids Res 44:7292–7303. https://doi.org/10.1093/nar/gkw602.
9. Gmuender H, Kuratli K, Di Padova K, Gray CP, Keck W, Evers S. 2001. Gene expression changes triggered by exposure of Haemophilus influenzae to novobiocin or ciprofloxacin: combined transcription and translation analysis. Genome Res 11:28–42. https://doi.org/10.1101/gr.157701.

10. Peter BJ, Arsuaga J, Breier AM, Khodursky AB, Brown PO, Cozzarelli NR. 2004. Genomic transcriptional response to loss of chromosomal supercoiling in Escherichia coli. Genome Biol 5:R87. https://doi.org/10.1186/gb-2004-5-11-r87.
11. Rui S, Tse-Dinh Y-C. 2003. Topoisomerase function during bacterial responses to environmental challenge. Front Biosci 8:d256–263. https://doi.org/10.2741/984.
12. Szafran MJ, Gongerowska M, Małecki T, Elliot M, Jakimowicz D. 2019. Transcriptional response of Streptomyces coelicolor to rapid chromosome relaxation or long-term supercoiling imbalance. Front Microbiol 10:1605. https://doi.org/10.3389/fmicb.2019.01605.
13. Webber MA, Ricci V, Whitehead R, Patel M, Fookes M, Ivens A, Piddock LJV. 2013. Clinically relevant mutant DNA gyrase alters supercoiling, changes the transcriptome, and confers multidrug resistance. mBio 4:e00273-13. https://doi.org/10.1128/mBio.00273-13.
14. Bouffartigues E, Buckle M, Badaut C, Travers A, Rimsky S. 2007. H-NS cooperative binding to high-affinity sites in a regulatory element results in transcriptional silencing. Nat Struct Mol Biol 14:441–448. https://doi.org/10.1038/nsmb1233.
15. Falconi M, Colonna B, Prosseda G, Micheli G, Gualerzi CO. 1998. Thermoregulation of Shigella and Escherichia coli EIEC pathogenicity. A temperature-dependent structural transition of DNA modulates accessibility of virF promoter to transcriptional repressor H-NS. EMBO J 17:7033–7043. https://doi.org/10.1093/emboj/17.23.7033.
16. Japaridze A, Renevey S, Sobetzko P, Stoliar L, Nasser W, Dietler G, Muskhelishvili G. 2017. Spatial organization of DNA sequences directs the assembly of bacterial chromatin by a nucleoid-associated protein. J Biol Chem 292:7607–7618. https://doi.org/10.1074/jbc.M117.780239.
17. Kar S, Adhya S. 2001. Recruitment of HU by piggyback: a special role of GalR in repressosome assembly. Genes Dev 15:2273–2281. https://doi.org/10.1101/gad.920301.
18. Ouafa Z-A, Reverchon S, Lautier T, Muskhelishvili G, Nasser W. 2012. The nucleoid-associated proteins H-NS and FIS modulate the DNA supercoiling response of the pel genes, the major virulence factors in the plant pathogen bacterium Dickeya dadantii. Nucleic Acids Res 40:4306–4319. https://doi.org/10.1093/nar/gks014.
19. Flärdh K, Buttner MJ. 2009. Streptomyces morphogenetics: dissecting differentiation in a filamentous bacterium. Nat Rev Microbiol 7:36–49. https://doi.org/10.1038/nrmicro1968.
20. Jones SE, Ho L, Rees CA, Hill JE, Nodwell JR, Elliot MA. 2017. Streptomyces exploration is triggered by fungal interactions and volatile signals. Elife 6:e21738. https://doi.org/10.7554/eLife.21738.
21. Szafran MJ, Jakimowicz D, Elliot MA. 2020. Compaction and control—the role of chromosome-organizing proteins in Streptomyces. FEMS Microbiol Rev 44:725–739. https://doi.org/10.1093/femsre/fuaa028.
22. Chater KF. 2001. Regulation of sporulation in Streptomyces coelicolor A32: a checkpoint multiplex? Curr Open Microbiol 4:667–673. https://doi.org/10.1016/s1369-5274(01)00267-3.
23. Kelemen GH, Buttner MJ. 1998. Initiation of aerial mycelium formation in Streptomyces. Curr Opin Microbiol 1:656–662. https://doi.org/10.1016/S1369-5274(98)80111-2.
24. Bush MJ. 2018. The actinobacterial WhiB-like (Wbl) family of transcription factors. Mol Microbiol 110:663–676. https://doi.org/10.1111/mmi.14117.
25. Bush MJ, Tschowri N, Schlimpert S, Flärdh K, Buttner MJ. 2015. c-di-GMP signalling and the regulation of developmental transitions in streptomycetes. Nat Rev Microbiol 13:749–760. https://doi.org/10.1038/nrmicro3546.
26. Romero-Rodríguez A, Robledo-Casados I, Sánchez S. 2015. An overview on transcriptional regulators in Streptomyces. Biochim Biophys Acta 1849:1017–1039. https://doi.org/10.1016/j.bbagrm.2015.06.007.
27. Shen X-L, Dong H-J, Hou X-P, Guan W-J, Li Y-Q. 2008. FtsY affects sporulation and antibiotic production by whiH in Streptomyces coelicolor. Curr Microbiol 56:61–65. https://doi.org/10.1007/s00284-007-9039-y.
28. van Wezel GP, van der Meulen J, Kawamoto S, Luiten RGM, Koerten HK, Kraal B. 2000. ssgA is essential for sporulation of Streptomyces coelicolor A3(2) and affects hyphal development by stimulating septum formation. J Bacteriol 182:5653–5662. https://doi.org/10.1128/JB.182.20.5653-5662.2000.
29. Xu D, Seghezzi N, Esnault C, Virolle M-J. 2010. Repression of antibiotic production and sporulation in Streptomyces coelicolor by overexpression of a TetR family transcriptional regulator. Appl Environ Microbiol 76:7741–7753. https://doi.org/10.1128/AEM.00819-10.
30. Chater KF. 2006. Streptomyces inside-out: a new perspective on the bacteria that provide us with antibiotics. Philos Trans R Soc Lond B Biol Sci 361:761–768. https://doi.org/10.1098/rstb.2005.1758.
31. Lu F, Hou Y, Zhang H, Chu Y, Xia H, Tian Y. 2017. Regulatory genes and their roles for improvement of antibiotic biosynthesis in Streptomyces. 3 Biotech 7:250. https://doi.org/10.1007/s13205-017-0875-6.
32. van der Meij A, Worsley SF, Hutchings MI, van Wezel GP. 2017. Chemical ecology of antibiotic production by actinomycetes. FEMS Microbiol Rev 41:392–416. https://doi.org/10.1093/femsre/fux005.
33. Urem M, Świątek-Połatyńska MA, Rigali S, van Wezel GP. 2016. Intertwining nutrient-sensory networks and the control of antibiotic production in Streptomyces. Mol Microbiol 102:183–195. https://doi.org/10.1111/mmi.13464.
34. Zhu H, Sandiford SK, van Wezel GP. 2014. Triggers and cues that activate antibiotic production by actinomycetes. J Ind Microbiol Biotechnol 41:371–386. https://doi.org/10.1007/s10295-013-1309-z.
35. Hutchings MI, Hoskisson PA, Chandra G, Buttner MJ. 2004. Sensing and responding to diverse extracellular signals? Analysis of the sensor kinases and response regulators of Streptomyces coelicolor A3(2). Microbiology (Reading) 150:2795–2806. https://doi.org/10.1099/mic.0.27181-0.
36. McLean TC, Wilkinson B, Hutchings MI, Devine R. 2019. Dissolution of the disparate: co-ordinate regulation in antibiotic biosynthesis. Antibiotics (Basel) 8:83. https://doi.org/10.3390/antibiotics8020083.
37. Rodríguez H, Rico S, Díaz M, Santamaría RI. 2013. Two-component systems in Streptomyces: key regulators of antibiotic complex pathways. Microb Cell Fact 12:127. https://doi.org/10.1186/1475-2859-12-127.
38. Szafran M, Skut P, Ditkowski B, Ginda K, Chandra G, Zakrzewska-Czerwińska J, Jakimowicz D. 2013. Topoisomerase I (TopA) is recruited to ParB complexes and is required for proper chromosome organization during Streptomyces coelicolor sporulation. J Bacteriol 195:4445–4455. https://doi.org/10.1128/JB.00798-13.
39. Donczew M, Mackiewicz P, Wróbel A, Flärdh K, Zakrzewska-Czerwińska J, Jakimowicz D. 2016. ParA and ParB coordinate chromosome segregation with cell elongation and division during Streptomyces sporulation. Open Biol 6:150263. https://doi.org/10.1098/rsob.150263.
40. Bentley SD, Chater KF, Cerdeño-Tárraga A-M, Challis GL, Thomson NR, James KD, Harris DE, Quail MA, Kieser H, Harper D, Bateman A, Brown S, Chandra G, Chen CW, Collins M, Cronin A, Fraser A, Goble A, Hidalgo J, Hornsby T, Howarth S, Huang C-H, Kieser T, Larke L, Murphy L, Oliver K, O'Neil S, Rabbinowitsch E, Rajandream M-A, Rutherford K, Rutter S, Seeger K, Saunders D, Sharp S, Squares R, Squares S, Taylor K, Warren T, Wietzorrek A, Woodward J, Barrell BG, Parkhill J, Hopwood DA. 2002. Complete genome sequence of the model actinomycete Streptomyces coelicolor A3(2). Nature 417:141–147. https://doi.org/10.1038/417141a.
41. Jeong Y, Kim J-N, Kim MW, Bucca G, Cho S, Yoon YJ, Kim B-G, Roe J-H, Kim SC, Smith CP, Cho B-K. 2016. The dynamic transcriptional and translational landscape of the model antibiotic producer Streptomyces coelicolor A3(2). Nat Commun 7:11605. https://doi.org/10.1038/ncomms11605.
42. Romero DA, Hasan AH, Lin Y-F, Kime L, Ruiz-Larrabeiti O, Urem M, Bucca G, Mamanova L, Laing EE, van Wezel GP, Smith CP, Kaberdin VR, McDowall KJ. 2014. A comparison of key aspects of gene regulation in Streptomyces coelicolor and Escherichia coli using nucleotide-resolution transcription maps produced in parallel by global and differential RNA sequencing. Mol Microbiol 94:963−987. https://doi.org/10.1111/mmi.12810.
43. Koskiniemi S, Lamoureux JG, Nikolakakis KC, t'Kint de Roodenbeke C, Kaplan MD, Low DA, Hayes CS. 2013. Rhs proteins from diverse bacteria mediate intercellular competition. Proc Natl Acad Sci U S A 110:7032–7037. https://doi.org/10.1073/pnas.1300627110.
44. Fu J, Qin R, Zong G, Zhong C, Zhang P, Kang N, Qi X, Cao G. 2019. The two-component system CepRS regulates the cephamycin C biosynthesis in Streptomyces clavuligerus F613-1. AMB Express 9:118. https://doi.org/10.1186/s13568-019-0844-z.
45. Liu M, Zhang P, Zhu Y, Lu T, Wang Y, Cao G, Shi M, Chen X-L, Tao M, Pang X. 2019. Novel two-component system MacRS is a pleiotropic regulator that controls multiple morphogenic membrane protein genes in Streptomyces coelicolor. Appl Environ Microbiol 85:e02178-18. https://doi.org/10.1128/AEM.02178-18.
46. Sola-Landa A, Moura RS, Martín JF. 2003. The two-component PhoR-PhoP system controls both primary metabolism and secondary metabolite biosynthesis in Streptomyces lividans. Proc Natl Acad Sci U S A 100:6133–6138. https://doi.org/10.1073/pnas.0931429100.
47. Zheng Y, Sun C-F, Fu Y, Chen X-A, Li Y-Q, Mao X-M. 2019. Dual regulation between the two-component system PhoRP and AdpA regulates antibiotic production in Streptomyces. J Ind Microbiol Biotechnol 46:725–737. https://doi.org/10.1007/s10295-018-02127-5.
48. Urem M, van Rossum T, Bucca G, Moolenaar GF, Laing E, Świątek-Połatyńska MA, Willemse J, Tenconi E, Rigali S, Goosen N, Smith CP, van Wezel GP. 2016. OsdR of Streptomyces coelicolor and the dormancy

regulator DevR of Mycobacterium tuberculosis control overlapping regulons. mSystems 1:e00014-16. https://doi.org/10.1128/mSystems.00014-16.
49. Chen S, Zheng G, Zhu H, He H, Chen L, Zhang W, Jiang W, Lu Y. 2016. Roles of two-component system AfsQ1/Q2 in regulating biosynthesis of the yellow-pigmented coelimycin P2 in Streptomyces coelicolor. FEMS Microbiology Lett 363:fnw160. https://doi.org/10.1093/femsle/fnw160.
50. Yu Z, Zhu H, Zheng G, Jiang W, Lu Y. 2014. A genome-wide transcriptomic analysis reveals diverse roles of the two-component system DraR-K in the physiological and morphological differentiation of Streptomyces coelicolor. Appl Microbiol Biotechnol 98:9351–9363. https://doi.org/10.1007/s00253-014-6102-z.
51. Rico S, Yepes A, Rodríguez H, Santamaría J, Antoraz S, Krause EM, Díaz M, Santamaría RI. 2014. Regulation of the AbrA1/A2 two-component system in Streptomyces coelicolor and the potential of its deletion strain as a heterologous host for antibiotic production. PLoS One 9:e109844. https://doi.org/10.1371/journal.pone.0109844.
52. Ortiz de Orué Lucana D, Groves MR. 2009. The three-component signalling system HbpS-SenS-SenR as an example of a redox sensing pathway in bacteria. Amino Acids 37:479–486. https://doi.org/10.1007/s00726-009-0260-9.
53. Kobayashi K, Ikemoto Y. 2019. Biofilm-associated toxin and extracellular protease cooperatively suppress competitors in Bacillus subtilis biofilms. PLoS Genet 15:e1008232. https://doi.org/10.1371/journal.pgen.1008232.
54. Rozas D, Gullón S, Mellado RP. 2012. A novel two-component system involved in the transition to secondary metabolism in Streptomyces coelicolor. PLoS One 7:e31760. https://doi.org/10.1371/journal.pone.0031760.
55. Hamoen LW, Werkhoven AFV, Venema G, Dubnau D. 2000. The pleiotropic response regulator DegU functions as a priming protein in competence development in Bacillus subtilis. Proc Natl Acad Sci U S A 97:9246–9251. https://doi.org/10.1073/pnas.160010597.
56. Kwon S-Y, Kwon H-J. 2013. The possible role of SCO3388, a tmrB-like gene of Streptomyces coelicolor, in germination and stress survival of spores. J Appl Biol Chem 56:165–170. https://doi.org/10.3839/jabc.2013.026.
57. Kim ES, Song JY, Kim DW, Chater KF, Lee KJ. 2008. A possible extended family of regulators of sigma factor activity in Streptomyces coelicolor. J Bacteriol 190:7559–7566. https://doi.org/10.1128/JB.00470-08.
58. Homerová D, Ševčíková B, Sprušanský O, Kormanec JY. 2000. Identification of DNA-binding proteins involved in regulation of expression of the Streptomyces aureofaciens sigF gene, which encodes sporulation sigma factor σF. Microbiology 146:2919–2928. https://doi.org/10.1099/00221287-146-11-2919.
59. Kormanec J, Homerová D, Potúcková L, Nováková R, Rezuchová B. 1996. Differential expression of two sporulation specific sigma factors of Streptomyces aureofaciens correlates with the developmental stage. Gene 181:19–27. https://doi.org/10.1016/S0378-1119(96)00395-2.
60. Feng X, Oropeza R, Kenney LJ. 2003. Dual regulation by phospho-OmpR of ssrA/B gene expression in Salmonella pathogenicity island 2. Mol Microbiol 48:1131–1143. https://doi.org/10.1046/j.1365-2958.2003.03502.x.
61. Soncini FC, Groisman EA. 1996. Two-component regulatory systems can interact to process multiple environmental signals. J Bacteriol 178:6796–6801. https://doi.org/10.1128/jb.178.23.6796-6801.1996.
62. Birkey SM, Liu W, Zhang X, Duggan MF, Hulett FM. 1998. Pho signal transduction network reveals direct transcriptional regulation of one two-component system by another two-component regulator: Bacillus subtilis PhoP directly regulates production of ResD. Mol Microbiol 30:943–953. https://doi.org/10.1046/j.1365-2958.1998.01122.x.
63. Cairns LS, Martyn JE, Bromley K, Stanley-Wall NR. 2015. An alternate route to phosphorylating DegU of Bacillus subtilis using acetyl phosphate. BMC Microbiol 15:78. https://doi.org/10.1186/s12866-015-0410-z.
64. Agrawal R, Sahoo BK, Saini DK. 2016. Cross-talk and specificity in two-component signal transduction pathways. Future Microbiol 11:685–697. https://doi.org/10.2217/fmb-2016-0001.
65. Desai SK, Kenney LJ. 2017. To ~P or not to ~P? Non-canonical activation by two-component response regulators. Mol Microbiol 103:203–213. https://doi.org/10.1111/mmi.13532.
66. Head CG, Tardy A, Kenney LJ. 1998. Relative binding affinities of OmpR and OmpR-phosphate at the ompF and ompC regulatory sites. J Mol Biol 281:857–870. https://doi.org/10.1006/jmbi.1998.1985.
67. Kenney LJ, Anand GS. 19 November 2020, posting date. EnvZ/OmpR two-component signaling: an archetype system that can function noncanonically. EcoSal Plus 9:10.1128/ecosalplus.ESP-0001-2019. https://doi.org/10.1128/ecosalplus.ESP-0001-2019.
68. Liu W, Hulett FM. 1997. Bacillus subtilis PhoP binds to the phoB tandem promoter exclusively within the phosphate starvation-inducible promoter. J Bacteriol 179:6302–6310. https://doi.org/10.1128/jb.179.20.6302-6310.1997.
69. Desai SK, Winardhi RS, Periasamy S, Dykas MM, Jie Y, Kenney LJ. 2016. The horizontally-acquired response regulator SsrB drives a Salmonella lifestyle switch by relieving biofilm silencing. Elife 5:e10747. https://doi.org/10.7554/eLife.10747.
70. Normanno D, Vanzi F, Pavone FS. 2008. Single-molecule manipulation reveals supercoiling-dependent modulation of lac repressor-mediated DNA looping. Nucleic Acids Res 36:2505–2513. https://doi.org/10.1093/nar/gkn071.
71. Norregaard K, Andersson M, Sneppen K, Nielsen PE, Brown S, Oddershede LB. 2013. DNA supercoiling enhances cooperativity and efficiency of an epigenetic switch. Proc Natl Acad Sci U S A 110:17386–17391. https://doi.org/10.1073/pnas.1215907110.
72. Cameron ADS, Dorman CJ. 2012. A fundamental regulatory mechanism operating through OmpR and DNA topology controls expression of Salmonella pathogenicity islands SPI-1 and SPI-2. PLoS Genet 8:e1002615. https://doi.org/10.1371/journal.pgen.1002615.
73. Fournier B, Klier A. 2004. Protein A gene expression is regulated by DNA supercoiling which is modified by the ArlS-ArlR two-component system of Staphylococcus aureus. Microbiology (Reading) 150:3807–3819. https://doi.org/10.1099/mic.0.27194-0.
74. Yao Y, Ma Y, Chen X, Bade R, Lv C, Zhu R. 2018. Absence of RstA results in delayed initiation of DNA replication in Escherichia coli. PLoS One 13:e0200688. https://doi.org/10.1371/journal.pone.0200688.
75. Sambrook J, Russell DW. 2001. Molecular cloning: a laboratory manual. CSHL Press, Cold Spring Harbor, NY.
76. Kieser T, Bibb MJ, Buttner MJ, Chater KF, Hopwood DA. 2000. Practical Streptomyces genetics. The John Innes Foundation, Norwich, United Kingdom.
77. Szafran MJ, Gongerowska M, Gutkowski P, Zakrzewska-Czerwińska J, Jakimowicz D. 2016. The coordinated positive regulation of topoisomerase genes maintains topological homeostasis in Streptomyces coelicolor. J Bacteriol 198:3016–3028. https://doi.org/10.1128/JB.00530-16.
78. Bilyk B, Weber S, Myronovskyi M, Bilyk O, Petzke L, Luzhetskyy A. 2013. In vivo random mutagenesis of streptomycetes using mariner-based transposon Himar1. Appl Microbiol Biotechnol 97:351–359. https://doi.org/10.1007/s00253-012-4550-x.
79. McClure R, Balasubramanian D, Sun Y, Bobrovskyy M, Sumby P, Genco CA, Vanderpool CK, Tjaden B. 2013. Computational analysis of bacterial RNA-Seq data. Nucleic Acids Res 41:e140. https://doi.org/10.1093/nar/gkt444.
80. Thorvaldsdóttir H, Robinson JT, Mesirov JP. 2013. Integrative Genomics Viewer (IGV): high-performance genomics data visualization and exploration. Brief Bioinform 14:178–192. https://doi.org/10.1093/bib/bbs017.
81. Robinson JT, Thorvaldsdóttir H, Winckler W, Guttman M, Lander ES, Getz G, Mesirov JP. 2011. Integrative Genomics Viewer. Nat Biotechnol 29:24–26. https://doi.org/10.1038/nbt.1754.
82. Seipke RF, Patrick E, Hutchings MI. 2014. Regulation of antimycin biosynthesis by the orphan ECF RNA polymerase sigma factor σ^{AntA}. PeerJ 2:e253. https://doi.org/10.7717/peerj.253.
83. RStudio Team. 2020. RStudio: integrated development environment for R. RStudio, PBC, Boston, MA.
84. Moody MJ, Young RA, Jones SE, Elliot MA. 2013. Comparative analysis of non-coding RNAs in the antibiotic-producing Streptomyces bacteria. BMC Genomics 14:558. https://doi.org/10.1186/1471-2164-14-558.